Charles University in Prague
Faculty of Mathematics and Physics

Jets in proton-proton and heavy ion collisions at the LHC

Martin Spousta

Habilitation Thesis for Associate Professor

March 2017

Acknowledgment

I'm grateful to my family and especially to my wife for their support and encouragement. My thank you should go to many people that I met during the journey partially imprinted in this thesis which is not possible to do properly. Thus, with providing no names, I'd like to thank to all my advisors, collaborators, students, and colleagues.

Contents

1 Prologue

Quarks, together with leptons, are basic building blocks of matter. At the present time, six quarks and six leptons are known. The interactions among these elementary constituents of matter are described by the theory called the Standard Model (SM) [1, 2, 3, 4, 5, 6, 7, 8, 9, 10]. The SM is a very successful theory which is capable of describing all the results from high-energy physics experiments up to date. The last discovered particle which was predicted by the SM is the Higgs boson. The Higgs boson was discovered by the ATLAS and CMS experiments at the Large Hadron Collider (LHC) in 2012 [11, 12, 13]. Despite the success of the SM, it is evident that this theory of elementary particles does not cover all the observed phenomena, namely it does not describe the physics of the dark matter and gravity. Consequently, the phenomena beyond SM are actively searched for at the LHC. Another problem of SM are limitations due to the perturbative description used in SM. These limitations imply that some aspects of the processes with elementary particles are very hard to calculate or describe. These aspects are generally called non-perturbative. One example of the non-perturbative process is hadronization. Hadronization is a process in which quarks, which are produced in a collision of elementary particles, turn into hadrons. This process is a consequence of a basic property of the strong interaction called confinement which prevents propagation of free quarks over large distances. When quarks are produced in the collision, they turn into hadrons after traveling a distance of the order of a femtometer. There is no rigorous theoretical description of this process and the space-time scales of this process are only roughly estimated. The question of transition of quarks to hadrons is one of the fundamental practical questions of physics.

The main motivation for colliding heavy ions is study of non-perturbative and collective properties of the strong interaction. This is being pursued via exploring the hot and dense nuclear matter created in these collisions. This hot and dense nuclear matter is composed of deconfined quarks and gluons. If a high-transverse momentum quark or gluon is produced in the heavy ion collision, then the mutual interaction of strongly interacting elementary particles can be studied. The high-transverse momentum quarks and gluons are detectable as jets, collimated sprays of hadrons produced from this initial quark or gluon. Constituents of jets interact with the deconfined medium which leads to a change of properties of jets which is called jet quenching phenomenon. The jet quenching is observed as a strong suppression of jet yields and a pronounced modification of the jet internal structure. This suppression is dominantly due to the radiation of high transverse momentum quarks or gluons when passing through the deconfined medium. Jet studies in proton-proton (pp) and heavy ion collisions at the LHC are the main topic of this habilitation thesis.

The thesis is organized as follows. The first section is the prologue. The second section provides a short introduction to the basic theoretical description of the strong interaction and to the physics of jets. The third section is the introduction to the physics of jet quenching and it includes a summary of jet quenching related results obtained with the ATLAS experiment. The fourth section puts jet results into the context of other run 1 results from the ATLAS heavy ion physics program. The short section number five provides a summary and outlook. My selected publications are included in section six that is organized according to the evolution of my engagement in the field which I will briefly describe now.

I joint the effort of preparation of the physics program of the ATLAS experiment at

the LHC in 2004. These preparation works included participation in the construction of a part of the ATLAS inner detector, various simulations, and development of algorithms suitable for the reconstruction and analysis of events with jets. This work was running with no appreciable external output for about six years. When the physics program of the LHC started in 2009, I was working on two topics. The first topic was understanding the interplay between the detector performance and the jet reconstruction in *pp* collisions. The second topic was a preparation of the software for the jet reconstruction in the heavy ion run. The work on the first topic led me to contribute to first publications on jets by the ATLAS experiment: the measurement of the inclusive jet cross-section in 7 TeV *pp* collisions [14] and the measurement of jet shapes [15]. These two early publications provided a first validation of perturbative chromodynamics in a new kinematic regime and helped to improve the Monte Carlo modeling of jets at the LHC as described in Section 2.2. From my personal perspective, they helped me to build the experience that I used later in heavy ions. These two publications together with one proceedings paper are included in Section 6. My work on the second topic was one of the building blocks of the publication on the first detection of the jet quenching at the LHC [16]. The main part of this publication was done in a team of two Ph.D. students, myself and Brain Cole from Columbia University who led our team. This observation paper, which has up to now more than 300 citations, can be considered a discovery of the jet quenching at the LHC and a first direct measurement of that phenomenon using fully reconstructed jets. This work was followed by the effort to characterize the jet energy loss by studying the inclusive jet yields [17, 18], jet internal structure [19], and neighbouring jet production [20]. Final results from these studies were published during the period 2013-2016 and I'm one of 1-8 main authors of these publications within the ATLAS Collaboration. These publications together with few more related publications where I'm one of main authors are included in Section 6.2.

In parallel with the physics program, we had to ensure to collect usable data on jets during the heavy ion runs and to make the jet reconstruction performing correctly even in the presence of a large background from the heavy ion underlying event. This need led me to develop high-level trigger for jets for the 2011 and 2015 runs. This work followed the development in the offline jet reconstruction which I started in 2006 and which was then later led by Aaron Angerami from Columbia University. The summary of the heavy ion jet trigger performance has been published in Ref. [21]. My experience with the underlying event subtraction was used in the development of a new method for the subtraction of large backgrounds from jets. This method was a first publicly available method which subtracts backgrounds at the level of jet constituents. This method may help also in the searches for beyond-SM particles in decays of boosted objects where a precise determination of the jet substructure is needed. This method is currently starting to be used by all three major LHC experiments and experiments at Relativistic Heavy Ion Collider (RHIC) at Brookhaven. The development of this method was led by Peter Berta and it was published in Ref. [22]. My publications on technical aspects of the jet reconstruction are collected in Section 6.3.

More recently, I started to work on the phenomenological aspects of the jet quenching aiming to interpret the data from LHC experiments [23, 24]. These publications are included in Section 6.4 and some context is provided in Section 3.3.

The general interest of the physics community in the physics discussed in this thesis can be illustrated by dedicated talks at international conferences. During the years 2008-2017,

I delivered 20 talks at various international conferences including four invited plenary talks. I'm including three selected proceedings into this thesis.

2 Jets in Quantum Chromodynamics

In this section I provide a short introduction to the Quantum Chromodynamics, the theory of strong interactions, and the concept of jet. I define basic terms such as coupling constant α_s, parton distribution functions or fragmentation functions that are used throughout this thesis. For more detailed reading I refer to classical textbooks [25, 26, 27, 28, 29] or a review [30].

2.1 Basic concept of Quantum Chromodynamics

Quantum Chromodynamics (QCD) is a quantum field theory with a *non-abelian gauge symmetry* group SU(3). The interaction among three color quark fields ψ_q^i and eight color gluon fields A_ν^a is described by the QCD Lagrangian

$$L^{\mathrm{QCD}} = -\frac{1}{4}F_{\mu\nu}^{(a)}F^{(a)\mu\nu} + \sum_q \bar{\psi}_{q,a}(i\gamma^\mu\partial_\mu\delta_{ab} - g_s\frac{\lambda^c}{2}A_\mu^c - m_q\delta_{ab})\psi_{q,b}, \quad (1)$$

$$F_{\mu\nu}^{(a)} = \partial_\mu A_\nu^a - \partial_\nu A_\mu^a - g_s f_{abc}A_\mu^b A_\nu^c. \quad (2)$$

Here g_s or $\alpha_s = g_s^2/4\pi$ is the QCD coupling constant, f_{abc} are the structure constants of SU(3) algebra, λ^a are the Gell-Mann matrices, and γ^μ are the Dirac γ-matrices. The $\psi_{q,a}$ are quark field spinors for a quark which has flavor q, mass m_q, and one of three colors a. The A_μ^a correspond to gluon fields where each massless gluon can have one of eight colors labeled by index a. The non-abelian character of the interaction leads to the presence of gluon self-interactions in the first term of the Lagrangian that are unique to QCD compared to Quantum Electrodynamics (QED). Instead of solving directly the equations of motion for the Lagrangian (1) which is impossible at the present time, the perturbation theory (pQCD) was developed to compute observable quantities determined by the short distance interaction of quarks and gluons. Each such observable quantity, R, can be then written as a series in α_s

$$R = r_0\alpha_s^k + r_1\alpha_s^{k+1} + ... \quad (3)$$

The coefficients r_i come from calculating contributions corresponding to appropriate Feynman diagrams.

QCD is an *asymptotically free gauge field theory*, which means that the coupling parameter α_s between the quarks and gluons becomes weaker in the short-distance limit. To explain this behavior of the strong force we refer to the concept of the renormalization. Generally, in the perturbative expansion of an observable, contributions from quantum loops may appear which diverge at large momenta. These divergent terms in the perturbative expansion can be absorbed into the redefinition of the coupling constant (or generally parameters of the Lagrangian). The original coupling constant α_s has to be replaced by an effective coupling that depends on the momentum scale Q^2. Such procedure is called renormalization. Then, to the first order in the perturbation series, the following relation between the coupling at different momentum scales Q_1^2 and Q_2^2 can be derived

$$\alpha_s(Q_2^2) = \frac{\alpha_s(Q_1^2)}{1 + \alpha_s(Q_1^2)\beta_0/4\pi \ln(Q_2^2/Q_1^2)}. \tag{4}$$

Since the theory only says what are the relative values of coupling parameter one must provide a "boundary condition" which fixes the absolute value of the coupling at certain momentum scale. In QED the value of coupling constant can be fixed to be the value of fine structure constant, $\alpha \approx 1/137$, at $Q^2 \to 0$ which is so called Thomson limit. In QCD it is not possible to use the same limit as will be clear from further discussion. Instead, roughly speaking, one can choose some value of Q^2, say $Q^2 = \mu^2$, compare experimental measurement of observable R with the theoretical calculation according to (3) and extract the value of $\alpha_s(\mu^2)$. The μ^2 that was chosen is called renormalization scale.

In general, any dimensionless physical quantity R that depends on transferred momentum Q^2 computed to a fixed order in pQCD will also depend on the scale μ^2 and on the renormalized coupling, $R = R(Q^2/\mu^2, \alpha_s(\mu^2))$. This means that the relation (3) should be written more precisely as

$$R = r_0\alpha_s^k(\mu^2) + r_1(Q^2/\mu^2)\alpha_s^{k+1}(\mu^2) + ... \tag{5}$$

However, after computing the observable R to all orders in perturbation theory, the observable cannot depend on the choice of μ^2 (even if practically it is not possible to compute the observable quantity to all orders). This means that the total derivative of R with respect to μ^2 is zero,

$$\mu^2 \frac{\mathrm{d}R}{\mathrm{d}\mu^2} = \left(\mu^2 \frac{\partial}{\partial \mu^2} + \mu^2 \frac{\partial \alpha_s}{\partial \mu^2}\frac{\partial}{\partial \alpha_s}\right) R = 0. \tag{6}$$

Here β-function can be introduced,

$$\beta(\alpha_s) \equiv \mu^2 \frac{\partial \alpha_s}{\partial \mu^2}, \tag{7}$$

and Eq. (7) is so-called renormalization group equation which tells us how a change of the scale μ is compensated by a change of the coupling α_s. The expansion of the β-function can be performed,

$$\frac{1}{\alpha_s}\beta(\alpha_s) = -\frac{\alpha_s}{4\pi}\beta_0 - \left(\frac{\alpha_s}{4\pi}\right)^2 \beta_1 - \left(\frac{\alpha_s}{4\pi}\right)^3 \beta_2 + O(\alpha_s^4), \tag{8}$$

where coefficients β_i depend on the number of quark flavors, n_f, color factors, and on the choice of the renormalization scheme which will be introduced in what follows. Solving the renormalization group equation at "i^{th} order" means to sum over diagrams with loops and to calculate β_i. At the leading order (LO) and next-to-leading order (NLO) $\beta_0 = 11 - 2/3n_f$ and $\beta_1 = 51 - 19/3n_f$, respectively. It is remarkable that for $n_f \leq 16$ the coefficient β_0 is *positive*. This is because the contribution from gluon loops dominates the contribution from quark loops. Positive values of β_0 leads to the fact that the QCD coupling constant vanishes at $\mu^2 \to \infty$ which is the fundamental phenomenon, called asymptotic freedom as mentioned above. Another important consequence is that at the LO the coupling constant diverges for $\mu^2 \to 0$, or more precisely at $\mu = \Lambda_{\text{QCD}} \simeq 200$ MeV. This implies that the perturbative

theory become useless in the region of small momentum transferred. This region is governed by the confinement which gives rise to hadrons, color-neutral objects.

As stated above, the coefficients β_i generally depend on the choice of the renormalization scheme. Renormalization scheme reflects the freedom in the renormalization procedure to choose what finite parts of the loop amplitude are included into the infinite part that renormalizes the coupling constant. While there is such a freedom, any change in β_i due to the choice of the renormalization scheme has to be accompanied by a change of coefficients r_i in (5) since they are related by (6). This ambiguity holds even if β-function is summed to all orders, contrary to R which is a physical quantity. Hence, the relation (8) is merely a definition of the coupling constant.

The dependence of measurable quantity R on the scale μ and scheme (through β_i) is a measure of our ignorance of uncalculated higher order terms. Thus, the (in)sensitivity of R to the variation of μ and β_i can provide a guideline for their choice. The years of experience has shown that a scale μ characteristic to the typical energy scale of the process would be the most appropriate choice (e.g. for the $e^+e^- \to$ hadrons processes at LEP the μ is set to M_{Z^0}). The most often used renormalization scheme is so called modified minimal subtraction scheme ("$\overline{\mathrm{MS}}$ scheme") where it is the divergent part plus an universal constant that are absorbed to the redefinition of the coupling.

The pQCD calculations describe very well processes even at quite low Q^2. Although one cannot theoretically, i.e. based on some convergence argument, estimate the lowest Q^2 accessible with perturbative calculations, below certain scale (of the order of a GeV) pQCD cannot describe the behavior of quarks and gluons. At such low transverse momenta the relevant degrees of freedom are not quarks and gluons but hadrons composed of these elementary particles. The dynamics of the transition from quarks and gluons to hadrons, i.e. so-called hadronization, is not known. This implies that initial and final state hadrons have to be characterized by non-perturbative methods. Consequently, for example the total cross-section characterizing the production of observed hadrons in hard hadron-hadron collisions can be factorized into three parts: parton distribution functions describing the initial state hadrons, cross-section for an elementary collision of quarks and gluons calculable perturbatively, and fragmentation function describing outgoing final state hadrons. Both, parton distribution functions and fragmentation functions are non-perturbative quantities. As an example, the cross-section for a production of a hadron h in proton-proton (pp) collisions can be written as

$$\frac{\mathrm{d}\sigma_{pp\to h}}{\mathrm{d}\hat{t}} = \sum_{\mathrm{abc}} \mathrm{d}x_a \mathrm{d}x_b f_{a/p}(x_a, M) f_{b/p}(x_b, M) \frac{\mathrm{d}\hat{\sigma}_{ab\to c}}{\mathrm{d}\hat{t}}(\hat{s}, \hat{t}, M, \mu) D_{c\to h}(z, p_T, M'). \quad (9)$$

where $f_{a/p}(x_a, M)$ is a parton distribution function for a quark or gluon a in the proton; $\hat{\sigma}$ is cross-section for an elementary collision of quarks and gluons (which depends on quantities $\hat{s}$ and $\hat{t}$ describing the kinematics of parton level collision); and $D_{c\to h}(z, p_T, M')$ is a fragmentation function. The scales M and μ correspond to scales at which we separate the hard, perturbative process from the initial and final-state evolutions, respectively. The scale μ is the renormalization scale. The scale M is called factorization scale. Meaning of M and x will be clarified in next paragraphs.

Parton distribution functions have been introduced in the Feynman's parton model

where, loosely speaking, the total momentum of the proton is a sum over the momenta of elementary "partons," i.e. quarks or gluons. Before the invention of the parton model, the cross-section of deep inelastic scattering of a lepton on hadron has been expressed in terms of form factors or structure functions of a hadron, $F(x, Q^2)$. It was experimentally observed that the structure functions approximately scale as function of transverse momentum Q^2, i.e. $F(x, Q^2)$ is independent of Q^2 in the kinematic region where Q^2 is sufficiently large (greater than few GeV^2) and x is fixed. This allowed to formulate the parton model where structure functions can be expressed as a sum of the parton distribution functions $f(x)$, characterizing the probability of finding a parton of charge e carrying a momentum fraction x of the whole proton momentum, i.e. $F(x) = x\Sigma_i e_i^2 f_i(x)$. The pQCD calculations which go beyond the LO predict a logarithmic deviations from the scaling that were later also experimentally measured. The reason for this breaking of the scaling is the fact that parton in the proton can emit a gluon, with a probability determined by α_s, and lose momentum as a result. The gluon emission brings collinear divergences that can be treated in a formally similar way as the renormalization of the coupling constant. Similarly to the running coupling renormalization, one can introduce a factorization scale M and express the parton distribution functions at a given factorization scale as a function of bare, divergent parton distribution function. It is not possible to calculate the parton distribution functions but it is possible to derive their scale dependence. This scale dependence is characterized by the Dokshitzer-Gribov-Lipatov-Altarelli-Parisi (DGLAP) evolution equations. The DGLAP evolution equation for the quark distribution function $q_i(x, M)$ can be written in the LO as

$$\frac{\partial q_i(y, M)}{\partial \ln M^2} = \frac{\alpha_s(M)}{2\pi} \left[\int_x^1 \frac{\mathrm{d}y}{y} P_{qq}\Big(\frac{x}{y}\Big) q_i(y, M) + \int_x^1 \frac{\mathrm{d}y}{y} P_{qg}\Big(\frac{x}{y}\Big) g(y, M) \right]. \tag{10}$$

Similar equations can be written for the anti-quark distribution function $\bar{q}_i(x, M)$, and gluon distribution function $g(x, M)$. Functions $P_{qq}(z)$ and $P_{qg}(z)$ in (10) represent leading order splitting functions, that describe the distribution of "daughter particles" carrying a fraction $z = x/y$ of their "mother's particle" momenta y. The factorization scale M represents a maximal virtuality of a last "daughter" particle in a subsequent splitting. Beyond the leading order the definition of parton distribution functions (like the definition of α_s) becomes also factorization scheme dependent. Factorization scheme is defined by a choice of higher order splitting functions. DGLAP evolution equations at the leading order (10) are an analogue of the renormalization group equation (8) at leading order. As said above, it is not possible to calculate parton distribution functions perturbatively. Their x dependence at some scale Q_0 has to be extracted from the experimental data. Generally, the parameterization of both, quark and gluon distribution functions have the following form

$$q/g(x, Q_0) = c_0 x^{c_1} (1 - x)^{c_2} f(x; c_3, ...), \tag{11}$$

where coefficients c_i are free parameters. Parameter Q_0 is a reference scale that must be chosen – usually $1 - 2$ GeV is used. The equation (11) with the values of coefficients c_i can be viewed as a boundary condition for the evolution equations (10). In practice, the values of coefficients c_i are extracted from a global fit of all available data at different Q^2. This is done by several working groups. The uncertainty of the parton distribution function is often large, namely in the region of x that is not well covered by kinematic capabilities of existing experiments. To quantify the uncertainty in the measured quantity related to the

uncertainty of the parton distribution functions, calculations of PDFs from different groups are typically used.

Final state observed hadrons are characterized by the fragmentation functions. While fragmentation functions are non-perturbative and model dependent, they are universal and once measured, e.g. in e^+e^- annihilation, they can be used to describe hadron production in other hard QCD processes. There are different models that describe the fragmentation process. The idea of the description of hadronization using the fragmentation functions originated from Feynman's independent fragmentation model. In that model, fragmentation function $D_{q\to h}(z, p_T, M')$ is a probability that a parton q (quark, anti-quark, "di-quark" or gluon) produces a hadron h, carrying a fraction z of the original parton energy and transverse momentum p_T. When integrating over all momenta fragmentation function gives the average number of hadrons coming from the fragmentation of a parton q. Similarly to the parton distribution functions, the fragmentation function depends implicitly also on the factorization scale M'.

2.2 Jets and their measurement

The most sensitive tests of pQCD have been provided by jet measurements. Jet is a collimated spray of hadrons (or their decay products) that come from a single parton created in a hard scattering. Thus, the energy of the jet is related to the energy of the original parton. The cross-section for a single jet production can be written, similarly to relation (9), as follows

$$\frac{\mathrm{d}\sigma_{pp\to\mathrm{jet}}}{\mathrm{d}p_T} = \sum_{\mathrm{abc}} \int\int\int_{p_{\mathrm{T,min}}^{\mathrm{jet}}}^{p_{\mathrm{T,max}}^{\mathrm{jet}}} \mathrm{d}x_a \mathrm{d}x_b \mathrm{d}\hat{t}\; f_{a/p}(x_a, M) f_{b/p}(x_b, M) \frac{\mathrm{d}\hat{\sigma}_{ab\to c}}{\mathrm{d}\hat{t}}(\hat{s}, \hat{t}, M, \mu) D(c \to \mathrm{jet}). \quad (12)$$

The $D(c \to \mathrm{jet})$ is not a single fragmentation function but rather a substitute for a complex algorithm that consists of a fragmentation algorithm (based on a particular fragmentation model) and a jet algorithm that defines which of the fragmentation products constitute the jet. An ideal jet algorithm would include all the fragmentation products that come from a parton a and exclude those that come from either other parton (such as hard gluon radiated at large angle from parton a) or other processes (such as initial state radiation). However, in reality this is not possible since one cannot unambiguously distinguish the hard parton from the soft and since once cannot compute the hadronization process directly from QCD. This implies that a jet is not defined uniquely but different jet algorithms exist that may deliver more or less different jets. Two basic types of jet algorithms exist. A cluster-type algorithm and a cone-type algorithm. A cone-type algorithm assumes a fixed, cone topology of a jet. A cluster-type algorithm assumes an ordering of the fragmentation products in energy or space. Both algorithms start with a list of "protojets," each protojet i carrying four-momentum p_μ^i. Protojet can be e.g. a cluster measured in the calorimeter, a track measured in the inner detector, or a stable particle coming from a simulation of the process using the Monte Carlo (MC) event generator. Instead of representing the four-momentum of the protojet as the energy plus three components of momentum, following four quantities are often used: transverse momentum p_T, rapidity y, azimuthal angle ϕ, and mass m. Rapidity is defined

as $y = 1/2\,\ln(E + p_z)/(E - p_z)$ and in the limit of $m \to 0$ it coincides with pseudorapidity, $\eta = -\ln\tan\vartheta/2$, where ϑ is the longitudinal angle. The distance between two protojets i and j is defined in terms of the opening angle, ΔR_{ij}, which is the distance in the $y \times \phi$ space,

$$\Delta R_{ij} = \sqrt{(y_i - y_j)^2 + (\phi_i - \phi_j)^2}. \tag{13}$$

Jet algorithms need a recombination strategy to combine two or more protojets to another protojet or finally to a jet. Several strategies exist, we mention two of them. The first strategy directly sums the four-momenta $p^k_\mu = \sum_i p^i_\mu$, which is called the four-momentum recombination scheme. The second strategy, so called E_{T}-recombination scheme, works for massless protojets and it uses transverse energy weighting of the position in $\eta \times \phi$ space,

$$\begin{aligned} E_{\mathrm{T}} &= \sum_{i\in\mathrm{jet}} E_{T,i}, \\ \eta &= \frac{1}{E_{\mathrm{T}}} \sum_{i\in\mathrm{jet}} E_{T,i}\eta_i, \\ \phi &= \frac{1}{E_{\mathrm{T}}} \sum_{i\in\mathrm{jet}} E_{T,i}\phi_i. \end{aligned} \tag{14}$$

The LHC experiments use primarily the first recombination strategy along with cluster type jet algorithm called *successive recombination algorithm.*

The successive recombination algorithm has one free parameter, the distance parameter, R, which determines the size of the resulting jet. Typically, R in the range of 0.2 to 1.0 is used. The algorithm works as follows:

- For each protojet define
$$d_i = p^{2p}_{T,i} R, \tag{15}$$
for each pair of protojets define
$$d_{ij} = \min(p^{2p}_{T,i}, p^{2p}_{T,j})\Delta R_{ij}. \tag{16}$$
- Find the smallest value of all d_i and d_{ij} and label it $d_{\min}$.
- If $d_{\min}$ is a d_{ij} recombine protojet i and j to a new protojet.
- If $d_{\min}$ is a d_i the corresponding jet i is complete and is removed from the list of protojets.
- Repeat all preceding steps until there is no more protojets on the list.

The successive recombination algorithm exists in three variants defined by the choice of p. For $p = 1$ one obtains k_t-algorithm [31, 32], for $p = 0$ one obtains Cambridge/Aachen algorithm [33, 34], and $p = -1$ defines the anti-k_t algorithm [35]. The advantage of all three algorithms is their infrared and collinear safety which means that they are not sensitive to

addition of particles with $E \to 0$ and to splitting of one particle into two softer particles which move in the same direction. These three algorithms however differ in the way how they recombine protojets. The k_t-algorithm recombines first soft protojets and then hard. On the contrary, the anti-k_t algorithm recombines from hard to soft. The recombination of Cambridge/Aachen is then purely geometrical. It is the anti-k_t algorithm which is used as a default jet reconstruction algorithm at the LHC. One advantage of this algorithm is that it delivers jets that are on average circular in $y \times \phi$ space and that have rather narrow distribution of number of constituents. This is helpful since it allows e.g. for easier calibration procedure. The stable shape of anti-k_t jets is due to the fact that the anti-k_t algorithm is not sensitive to a presence of low p_T particles in the jet periphery which are coming from the underlying event (UE). This is not the case for the k_t-algorithm for which the number of constituents effectively depends on the magnitude of UE. This disfavors the use of the k_t-algorithm.

Jets are tools for performing detailed checks of the Standard Model as well as for searching for physics beyond the Standard Model. On the QCD front, jets may be used to test the level of accuracy of fixed order pQCD calculations, to extract the parton distribution functions as well as to access the magnitude of α_s. There are two basic QCD measurements with jets. These are the measurement of the inclusive jet cross-section and the measurement of jet shapes. The first inclusive jet cross-section measurement by ATLAS was published in Ref. [14] included in Section 6. In that publication, inclusive jet and the dijet cross-sections were measured in pp collisions with center-of-mass energy, $\sqrt{s}$, of 7 TeV for $R = 0.4$ and $R = 0.6$ anti-k_t jets. The total integrated luminosity of 17 nb^{-1} was used in this first measurement delivering jet spectra which reached up to $p_T \approx 600$ GeV. The jets were selected to have $p_T > 60$ GeV and rapidity $|y| < 2.8$. The measured cross section was compared with NLO QCD calculations corrected for non-perturbative effects. It was shown that the NLO predication agrees well with the data which provided a first validation of pQCD in a new kinematic regime of the LHC.

The first measurement of the jet shapes performed by ATLAS was published in Ref. [15] included in Section 6. Jet shapes were measured in pp collisions with $\sqrt{s} = 7$ TeV for $R = 0.6$ anti-k_t jets in the kinematic region 30 GeV $< p_T <$ 600 GeV and $|y| < 2.8$. The internal structure of jet is primarily dictated by the emission of multiple gluons from the primary parton, which is calculable in pQCD. The jet shape is sensitive to the flavor of the initial parton which was quantified in the measurement by comparison with MC generators. The jet shape is also sensitive to the non-perturbative fragmentation effects and UE contributions from the interaction between proton remnants. A proper modeling of these soft contributions is crucial for the understanding of jet production in hadron-hadron collisions and for unbiased comparisons of cross-sections involving jets with theoretical calculations.

Since these first measurements were done, many other results on QCD with jets were obtained by LHC experiments. The first two measurements discussed here are important not only for pQCD physics in pp collisions but also they were important as they provided a benchmark for measurements in heavy ion collisions that will be discussed in the next section.

3 Jet quenching phenomenon

In this section I provide a basic introduction to the physics of jet quenching. Section 3.1 provides a summary of the first experimental evidences for the jet quenching from experiments at Relativistic Heavy Ion Collider (RHIC). Section 3.2 provides a summary of results on the jet quenching delivered by the ATLAS experiment at the LHC. I include in the text only few selected figures and a basic description of results. Full set of selected results is included in Section 6.2. More general overview of the LHC jet quenching results is provided in Ref. [36] also included in Section 6.2. Finally, Section 3.3 summarizes basic theoretical concepts of the jet quenching.

Before starting with the physics results, we need to briefly introduce some of the basic quantities used in the heavy ion physics. First of the key quantities is the centrality of the collision. Centrality quantifies the overall level of activity or particle production in the collision. It can be expressed in terms of cumulative fraction of events (percentiles of the total number of events) with e.g. a total energy deposited in forward calorimeters in a certain range of values. As a result of convention, the lowest percentiles (e.g. 0–10%) always label events with the largest deposits in the forward calorimeters that is events with the largest event activity. The overall event activity reflects the degree of overlap of two colliding nuclei. Large event activity means large degree of the overlap of two colliding nuclei that is a small impact parameter. The degree of overlap of two colliding nuclei can be quantified also by the number of nucleons that participate in the collision, $N_{\rm part}$, that is the number of nucleons that suffer at least one inelastic collision. This quantity is determined in a geometrical model of the nucleus-nucleus collision called Glauber model [37, 38, 39]. In central events (e.g. the centrality percentile 0–10%) there is a large number of participants (at the LHC $N_{\rm part} \approx 350$), in peripheral events (e.g. the centrality percentile 60–80%) the number of participants is the smallest (at the LHC $N_{\rm part} \approx 20$). One can then also define the number of collisions, $N_{\rm coll}$, which is a number of binary nucleon-nucleon collisions.

3.1 First experimental evidence of jet quenching

Collisions of heavy-ions at ultra-relativistic energies can produce hot and dense colored medium where relevant degrees of freedom are not complex hadrons but deconfined quarks and gluons. This is a consequence of the asymptotic freedom of QCD. The dense colored medium created in these collisions is often called Quark-Gluon Plasma (QGP). One of the key signatures of QGP is its opaqueness to high-energy quarks and gluons, known as jet quenching. The jet quenching is a result of the energy loss of high-p_T partons that traverse the deconfined medium. The jet quenching was first proposed by Bjorken in 1982 [40] as an experimental tool to investigate properties of QGP. First observations of the jet quenching were done by experiments at RHIC. Main observations from RHIC were summarized in so-called white papers [41, 42, 43, 44]. Since the energy regime at RHIC does not easily allow studies of fully reconstructed jets, the single charged particles have been studied first. The basic observable that characterized these indirect measurements of the jet quenching is the nuclear modification factor of charged particles, R_{AB}. Generally, the nuclear modification factor is defined as a ratio of invariant yield in A+B collisions to that of pp, scaled by the average number of binary nucleon-nucleon collisions, $\langle N_{\rm coll} \rangle$ [45, 46],

$$R_{AB}(p_T) = \frac{\dfrac{1}{N_{\rm evnt}}\dfrac{{\rm d}^2N_{\rm A+B}}{{\rm d}\eta{\rm d}p_T}}{\dfrac{\langle N_{\rm coll}\rangle}{\sigma_{pp}^{\rm inel}}\dfrac{{\rm d}^2\sigma_{pp}}{{\rm d}\eta{\rm d}p_T}}. \quad (17)$$

Here $\sigma_{pp}^{\rm inel}$ is the total inelastic pp cross-section, $N_{\rm A+B}$ is the yield measured in A+B collisions which is due to a hard scattering process under the study, and σ_{pp} is the pp cross section for that process. The $\langle N_{\rm coll}\rangle$ is calculated using Glauber model [37, 38, 39]. The nuclear modification factor R_{AB} is constructed such that $R_{AB} = 1$ in the absence of nuclear modifications to the hard scattering.

Before summarizing the results from gold-gold (Au+Au) collisions where QGP was expected to be formed, it is useful to summarize basic results from deuteron-gold (d+Au) collisions where the energy released during the collision was expected not to be sufficient for the QGP formation. The d+Au collisions can be used as a reference to understand the effects seen in Au+Au collisions as well as to study the impact of nuclear modifications of parton distribution functions or other phenomena that are related to initial state effects. The left panel of Fig. 1 shows R_{dA} as a function of transverse momentum for d+Au collisions which characterizes the difference between the yields of charged particles in d+Au and pp collisions [47]. The R_{dA} is below unity for the smallest p_T and exceeds the unity for the majority of measured p_T values. Two main effects contribute here – Cronin effect and shadowing. The Cronin effect is responsible for the enhancement seen in R_{pA} or R_{dA} at moderate $p_T \gtrsim 2$ GeV [48]. This enhancement of yields can be understood as a consequence of multiple scattering of incoming partons/hadrons while passing through the target nucleus. These multiple scatterings happen prior to the hard scattering that produces a high-p$_T$ parton which then fragments into the observed hadrons. The second effect, shadowing, is related to the observation that R_{pA} or R_{dA} at low $p_T \lesssim 1-2$ GeV is less than one. This suppression is ascribed to the fact that the nucleons on the surface of the nucleus "shadow" (in an optical analogy) the inner nucleons which are thus not exposed to the full hadron beam intensity. This means that the effective number of nucleons participating in the inelastic interactions is reduced to the number of surface nucleons, i.e. $\sim A^{2/3}$ [49, 50]. Both of these effects are initial state effects which means that to account for them one needs to modify a description of processes happening before the hard scattering compared to the description in pp collisions. Most commonly, this is done within a factorized QCD cross-section (9) by using nuclear parton distribution functions [50, 51].

The $R_{dA}(p_T)$ can be compared with the $R_{AA}(p_T)$ measured in central Au+Au collisions. At $p_T > 4$ GeV, hadrons produced in central Au+Au collisions are suppressed by a factor of ~ 5 compared to the binary scaling expectation. This suppression extends up to $p_T \sim 10$ GeV. This observation could not be explained as an initial state effect and it was one of the first indirect evidences for a strong jet quenching in heavy ion collisions. An important direct check of the correctness of this interpretation is the measurement of the $R_{\rm AA}$ of prompt photons [52] which is consistent with unity. This is important since photons do not interact strongly and thus cannot be quenched. Another indirect evidence of the jet quenching was provided by the measurement of the dihadron azimuthal correlations which quantifies the azimuthal correlation between a trigger hadron within $4 < p_{\rm T}^{trig} < 6$ GeV and another hadron having 2 GeV $< p_T < p_{\rm T}^{trig}$ [53, 47]. The result of that analysis is shown in the right

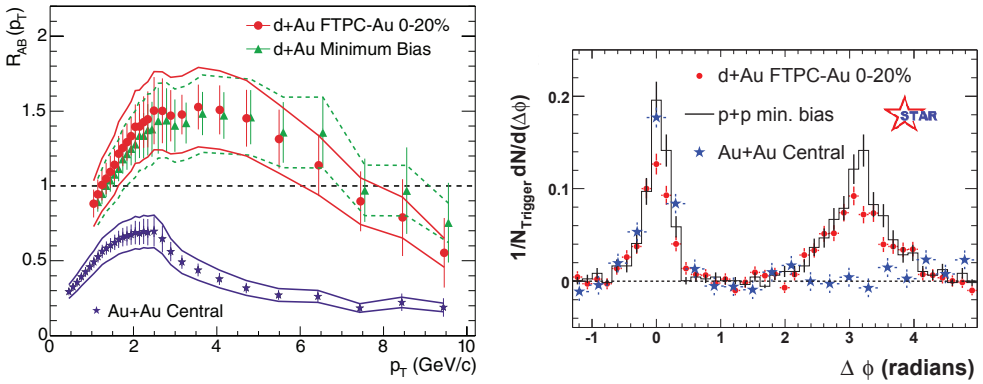

Figure 1: Left: R_{AB} as a function of p_T for central Au+Au collisions (blue stars) and d+Au collisions (red circles and green triangles), measured by STAR experiment. Right: Dihadron azimuthal correlations in *pp*, d+Au and Au+Au collisions. Both figures taken from Ref. [47].

panel of Fig. 1. One can see that a hadron pair drawn from a single jet generates an enhanced correlation at $\Delta\phi \simeq 0$ in *pp*, d+Au and Au+Au collisions. Then, a back-to-back hadron pair drawn from a dijet also generates an enhanced correlation at $\Delta\phi \simeq \pi$, which is observed for *pp* and d+Au collisions. On the contrary, such a correlation is completely absent in central Au+Au collisions which suggests a strong jet quenching. One advantage of this measurement is that it does not require the Glauber model to scale the yields and consequently it provides an evidence for the jet quenching which is complementary to measurements of $R_{\rm AA}$. These observations triggered a lot of attention and many other studies were done (see [41, 42, 43, 44]). Only very recently, the first result on fully reconstructed jets in Au+Au collisions appeared [54] which goes in the direction of LHC measurements that we will describe in the next section.

3.2 Jet quenching measurements by the ATLAS experiment

While a full jet reconstruction at RHIC is possible, limiting statistics and large signal-to-background ratios make measurements with fully reconstructed jets difficult to perform and generally less precise. Thus, the first direct observation of the jet quenching came from a measurement at the LHC. It was the measurement of the dijet asymmetry published in Ref. [16] included in Section 6.2. The dijet asymmetry was defined as $A_J = (E_{T,1} - E_{T,2})/(E_{T,1} + E_{T,2})$ where $E_{T,1}$ ($E_{T,2}$) is the transverse energy of the leading (sub-leading) jet. The sub-leading jet was defined to be the highest E_T jet located in the opposite hemisphere with respect to the leading jet, i.e. the azimuthal distance between the leading and sub-leading jet is $\Delta\phi > \pi/2$. The main result of the study is shown in Fig. 2. The results showed a significant increase of the number of events with large dijet asymmetry in central compared to peripheral collisions. Simultaneously to the dijet asymmetry, the dijet azimuthal correlation was also measured. No strong modification of the dijet azimuthal correlation was observed. This observation implies that the sub-leading jet is not deflected by the medium. From a technical point of view, it also implies that the jet reconstruction delivers real dijet events and not false, unphysical correlations. Recently, the dijet asymmetry measurement was updated [55] by providing the distributions fully corrected for the

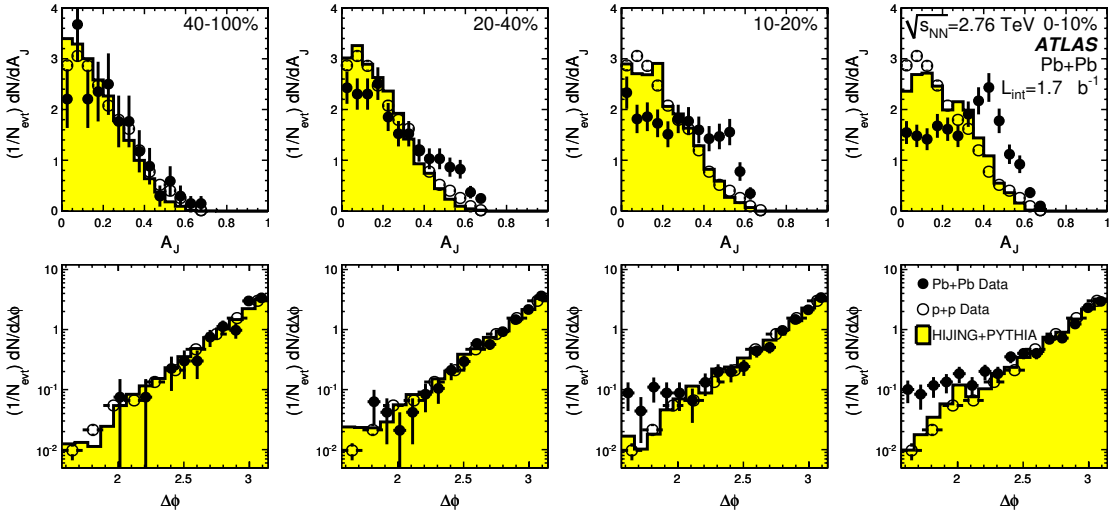

Figure 2: Top: Dijet asymmetry distributions for data (solid points) and MC (yellow histograms), as a function of collision centrality (left to right from peripheral to central events). Shown also are *pp* data from $\sqrt{s} = 7$ TeV collisions analyzed with the same jet selection (open circles). Bottom: Distribution of $\Delta\phi$, the azimuthal angle between the two jets, for data and MC, also as a function of centrality. Figure taken from Ref. [16].

detector effects. The results were obtained by measuring the two-dimensional $p_{T,1} - p_{T,2}$ distributions and applying an unfolding procedure to account for experimental resolution in the measurement of transverse momenta of both jets simultaneously. Resulting distributions are found to differ significantly between central collisions and peripheral or *pp* collisions. In particular, a maximum in the $p_{T,1}/p_{T,2}$ distribution was seen in 0–10% central collisions at a value of $p_{T,1}/p_{T,2} \approx 0.55$ for jets with $p_T = 100 - 126$ GeV. These results may help to constrain the role of fluctuations in the jet quenching and the path-length dependence of the energy loss.

The dijet asymmetry does not allow to distinguish events where both jets lose a similar amount of energy from those where the jets lose no energy. To overcome this, one naturally needs to study the inclusive jet spectra. Any effect of the jet quenching must exhibit itself in the change of the jet yields. To be able to directly compare jet yields measured in central to those measured in peripheral collisions one has to account for a different overlap of two colliding nuclei in central and peripheral collisions. This is done by normalizing the yields by $\langle N_{\rm coll} \rangle$ introduced in Section 3.1. After normalizing by $\langle N_{\rm coll} \rangle$ one can calculate the ratio of jet yields in central to peripheral collisions known as $R_{\rm CP}$,

$$R_{\rm CP} = \left(\frac{1}{N_{coll}^{\rm cent}} \frac{1}{N_{evts}^{\rm cent}} \frac{{\rm d}N_{jet}^{\rm cent}}{{\rm d}E_T} \right) \Big/ \left(\frac{1}{N_{coll}^{60-80\%}} \frac{1}{N_{evts}^{60-80\%}} \frac{{\rm d}N_{jet}^{60-80\%}}{{\rm d}E_T} \right),$$
$$\text{cent} \in \{0-10\%, 10-20\%, 20-30\%, 30-40\%, 40-50\%, 50-60\%\}. \quad (18)$$

The $R_{\rm CP}$ measured for $R = 0.2, 0.3, 0.4$, and 0.5 anti-k_t jets as a function of the centrality and transverse energy was published in Ref. [17] which is included in Section 6.2. The input jet yields were corrected for the detector effects using the SVD unfolding [56]. The

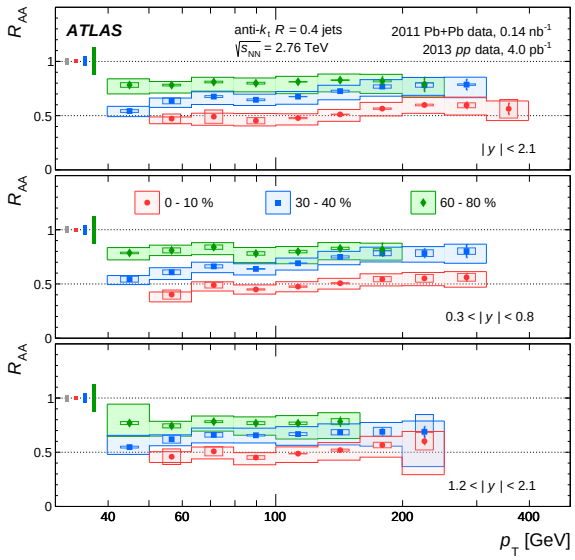

Figure 3: Jet R_{AA} as a function of p_T in different centrality bins with each panel showing a different range in $|y|$. The boxes, bands, and error bars indicate uncorrelated systematic, correlated systematic, and statistical uncertainties, respectively. Figure taken from Ref. [18].

R_{CP} decreases monotonically from peripheral to central collisions. In central collisions the jet yield is suppressed by about a factor of two with the suppression not exhibiting any strong dependence on the jet transverse energy. Suppression of jets with larger R is generally smaller when evaluated within the same E_T interval. This indicates that the lost energy is being redistributed outside of the jet cone rather than inside the jet cone. This conclusion is confirmed by a precise measurement of jet fragmentation [19, 57, 58] and the measurement of transverse energy flow in the event done by CMS [59].

These first measurements of jet suppression [16, 17] were followed by a precise measurement of the jet nuclear modification factor, R_{AA}, which was evaluated as a function of centrality, jet p_T, and jet rapidity. This measurement was published in Ref. [18] included in Section 6.2. The basic result of this measurement is included in Figure 3. The jet yields were measured over the kinematic range of jet transverse momentum $32 < p_T < 500$ GeV, and absolute rapidity $|y| < 2.1$. The jet R_{AA} was found to reach a value of approximately 0.5 implying that the jet yields are suppressed by a factor of two in central collisions compared to pp collisions. The R_{AA} shows a slight increase with p_T and no significant variation with rapidity. This later observation is particularly striking given the large differences in slopes of jet spectra and differences in the jet flavor at different rapidities. Also striking is relatively sizable modification seen in 60–80% peripheral collisions with the $R_{\mathrm{AA}} \approx 0.8$ for jets with $p_T < 100$ GeV.

A high-precision measurements of jet R_{AA} is only possible with a good understanding of the detector response, in particular the jet energy scale (JES) which was elaborated in Ref. [60] included in Section 6.2 of this thesis. The JES was constructed by calibrating the heavy ion (HI) jets with respect to the standard pp jets using the analysis of pp collision data. The JES for the latter is well understood through a combination of *in situ* techniques

in which the transverse momentum balance between a jet and a reference object such as a Z boson or γ was measured. To establish a JES calibration for the HI jets, pp data at $\sqrt{s} = 8$ TeV recorded in 2012 were analyzed and both pp and HI jets were reconstructed. The pp jets were then used as a reference to cross calibrate the HI jets. Applying the HI JES in data from different run periods requires to further consider the effects of different detector operating conditions as well as the fact that the flavor fractions are expected to change with the beam energy. An uncertainty on the absolute JES was derived for HI jets resulting from the "baseline" uncertainty on the reference jets, additional uncertainties in the cross calibration procedure itself, the flavor composition, and response uncertainties of HI jets. Finally, differences in the response to quenched jets were evaluated and a systematic uncertainty which accounts for such differences was derived using the PYQUEN [61] sample. The PYQUEN generator was setup to run in two different configurations chosen to match the modifications of fragmentation functions measured in the data. The total JES uncertainty in central Pb+Pb collisions was found to be largest at low p_T, approximately 4% at 30 GeV, and decreasing with p_T to values between $2-3\%$ at 450 GeV.

A complementary measurement to the jet $R_{\rm AA}$ is the $R_{\rm AA}$ of charged particles [62]. In that analysis, the charged particle spectra were measured over a wide transverse momentum range, $0.5 < p_T < 150$ GeV, and in eight bins of pseudorapidity covering the range of $|\eta| < 2$. The charged particle $R_{\rm AA}$ shows a distinct p_T dependence with a pronounced minimum at about 7 GeV. Above 60 GeV, $R_{\rm AA}$ is consistent with a plateau at a centrality-dependent value which is approximately 0.55 for the 0–5% most central collisions. The $R_{\rm AA}$ distribution is consistent with flat pseudorapidity dependence over the whole transverse momentum range in all centrality classes.

Since inclusive charged particles measured at different transverse momenta come from jets of different original energies, there is no simple mapping between the modified charged particle yields and the modification of the jet internal structure. Thus, our understanding of the jet quenching should strongly profit from the direct measurement of jet fragmentation which was published in Ref. [19] included in Section 6.2. In that measurement, it was found that the central-to-peripheral ratios of fragmentation functions of jets with $p_T > 100$ GeV show a reduction of fragment yield in central collisions relative to peripheral collisions at intermediate z values, $0.04 < z < 0.2$ and an enhancement in fragment yield for $z < 0.04$. A smaller, less significant enhancement was observed at large z in central collisions. These trends are shown in Figure 4. Similar observations as for the fragmentation functions were done also for the distributions of transverse momenta of charged particles reconstructed inside jets. From the analysis of measured distributions it was concluded for the 0–10% most central collisions that the increase in the number of particles with $0.02 < z < 0.04$ is less than one particle per jet. A decrease of about 1.5 particles per jet was observed for $0.04 < z < 0.2$. Further it was concluded that in the 0–10% most central collisions a small fraction, <2%, of the jet transverse momentum is carried by the excess particles in $0.02 < z < 0.04$ but the depletion in fragment yield in $0.04 < z < 0.2$ accounts on average for about 14% of jet p_T. This implies that the energy is redistributed to particles with $p_T < 2$ GeV. Recently, the dependence of the jet fragmentation on the jet p_T and rapidity was explored, see Refs. [63, 57]. These detailed measurements should directly help to improve understanding of modifications of parton showers in the medium.

To improve understanding of the path length dependence of the jet quenching and the

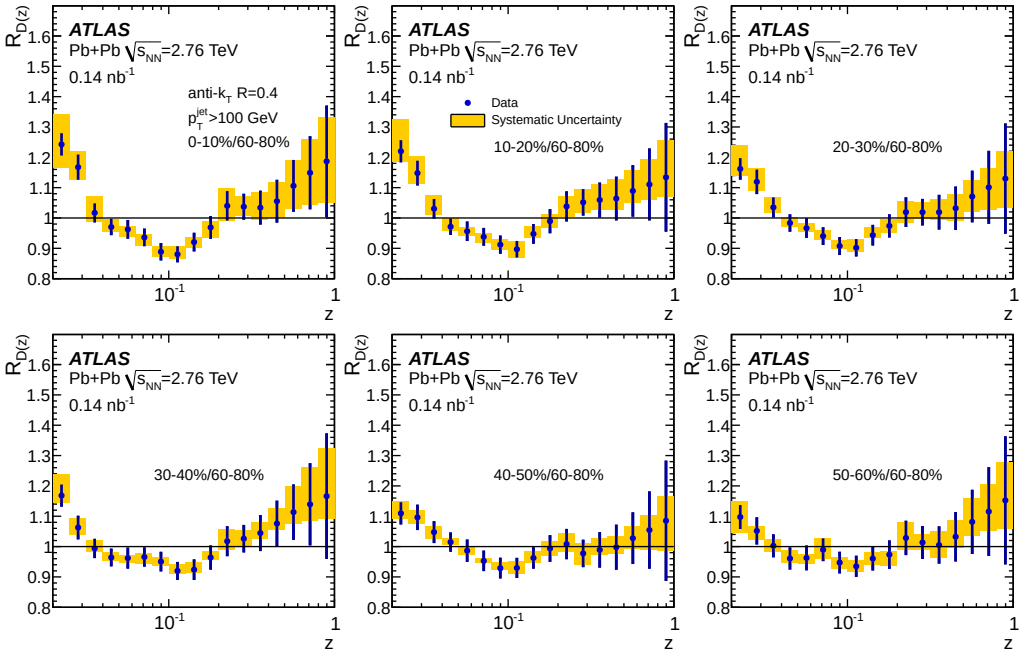

Figure 4: Ratios of fragmentation functions for six bins in collision centrality to those in peripheral (60–80%) collisions, $R_{D(z)}$, for $R = 0.4$ jets. The error bars on the data points indicate statistical uncertainties while the yellow shaded bands indicate systematic uncertainties. Figure taken from Ref. [19].

role of fluctuations in the jet quenching, three more differential measurements have been performed: the measurement of azimuthal dependence of inclusive jet yields [64] and more recently the measurement of correlation between dijet asymmetry and event-shape variables [65] and the measurement of neighbouring jet production [20]. The results of these three measurements are described in the next paragraphs and the last of these three publications is included in Section 6.2.

In the measurement of the azimuthal dependence of inclusive jet yields, the variation of inclusive jet suppression as a function of relative azimuthal angle, $\Delta\phi$, with respect to the elliptic event plane [66] was measured for jets with $p_T > 45$ GeV in six different collision centrality bins. The variation of the jet yield with $\Delta\phi$ was characterized by the parameter, $v_2^{\rm jet}$, and the ratio of out-of-plane ($\Delta\phi \sim \pi/2$) to in-plane ($\Delta\phi \sim 0$) yields. Non-zero $v_2^{\rm jet}$ values were measured in all centrality bins for jets with $p_T < 160$ GeV. The jet yields were observed to vary by as much as 20% between in-plane and out-of-plane directions and a significant $v_2^{\rm jet}$ of $2-5\%$ was observed even at very large jet p_T. This $v_2^{\rm jet}$ is a direct measure of the differential energy loss suffered by hard partons as they traverse different path-lengths of the medium in events characterized by the same collision centrality.

Motivated by $v_2^{\rm jet}$ measurements, a similar analysis was performed for the dijet asymmetry. The dijet asymmetry, $A_{\rm J}$, was studied as a function of angle between the leading-jet and the elliptic event-plane. These measurements effectively study the path-length dependence of $A_{\rm J}$ by requiring the jet pair to traverse different lengths of the medium. The dependence of the $\langle A_{\rm J}\rangle$ on the event-plane angle was quantified by calculating the second Fourier coefficient of the $\langle A_{\rm J}\rangle$ azimuthal distribution, termed c_2. The measured c_2 signal is quite

small ($\leq$2%), however, it is consistently negative, indicating a slightly larger asymmetry when the dijet pair is oriented out-of-plane than in-plane. This measurement was further extended by repeating the analysis when constraining the shape of the collision geometry by selecting events based on the magnitude of the second-order flow harmonic quantified by the magnitude of the q_2 vector. Within a given centrality interval, events with large q_2, i.e. events with a more elliptic geometry, show an increase in the c_2 for 20–30% and 30–40% centrality bins. In other centrality intervals, the statistical precision of the results, obtained with additional binning in q_2, is insufficient to conclude the observation of any systematic dependence of $\langle A_{\rm J} \rangle$ on the event-plane angle.

To further constrain the energy loss models, the measurement of the correlations between jets that are separated by small relative angles was performed. The measured neighbouring jet pairs result primarily from hard radiation by the parton that occurs early in the process of the shower formation. Generally, two neighbouring jets originating from the same hard scattering should have more similar path lengths in the medium compared to the two jets in the dijet measurements. Therefore measuring neighbouring jets could probe differences in their quenching that do not result primarily from difference in path length as well as put some constraints to models in which a part of the parton shower radiates coherently in the response to the medium. The production of pairs of correlated jets was quantified using the rate of neighbouring jets that accompany a test jet, $R_{\Delta R}$. This observable was used in past by D$\emptyset$ collaboration to measure the strong coupling constant, α_s, and to test its running over a large range of transverse momenta [67]. The $R_{\Delta R}$ was evaluated both as a function of test-jet E_T and neighbouring-jet E_T. A significant dependence of $R_{\Delta R}$ on collision centrality was observed in both cases, suggesting a suppression of neighbouring jets which increases with increasing centrality of the collision. The centrality dependence of the suppression was further quantified using the central-to-peripheral ratio of $R_{\Delta R}$ distributions, $\rho_{R_{\Delta R}}$. The trends seen in $\rho_{R_{\Delta R}}$ evaluated as a function of neighbouring-jet E_T indicate a decrease in suppression with increasing neighbouring-jet E_T. The $\rho_{R_{\Delta R}}$ evaluated as a function of test-jet E_T exhibits a suppression reaching values of $0.5 - 0.7$ in 0–10% central collisions and does not show any strong dependence on E_T.

The weak c_2 signal for the dijet asymmetry, the significant single jet v_2 and characteristic behavior seen in the neighbouring jet production can provide strong constraints on the path length dependence of the energy loss.

3.3 Theoretical description of jet quenching

The idea of the energy loss of jets propagating through the dense partonic medium was proposed by Bjorken in early eighties [40] as mentioned in Section 3.1. Bjorken's arguments were based on elastic scattering of high momentum partons from quanta in the medium which results in an ionization-like energy loss. Since then, it has been found that even if the collisional energy loss may contribute, particularly in the case of the energy loss of heavy quarks [68], the main source of the parton energy loss is gluon radiation. The gluon radiation in the deconfined QCD matter is similar to the bremsstrahlung process in QED. Hard scattered parton on its path through the medium can scatter off and radiate gluons that may subsequently interact with the medium. In this section we will provide a basic introduction to the description of the parton energy loss. Detailed reviews are provided in

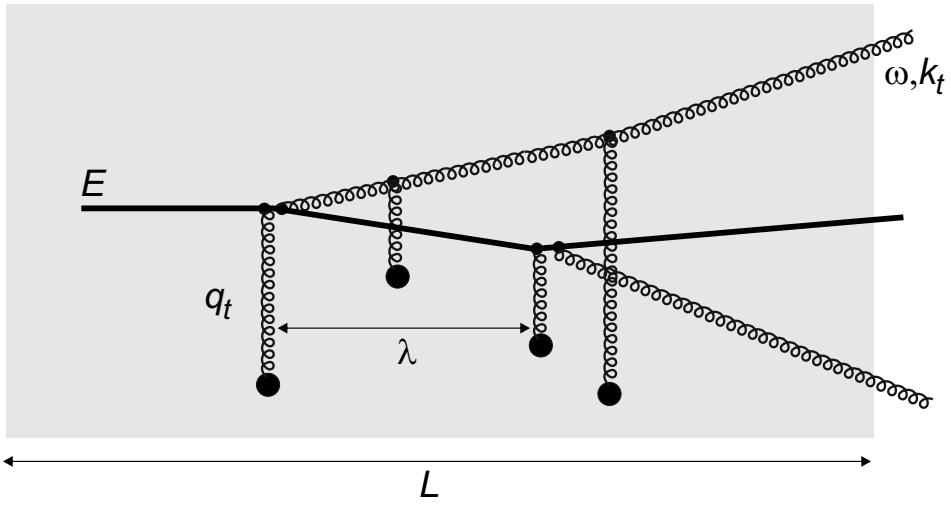

Figure 5: Sketch of the medium-induced gluon radiation (for details see the text). (Courtesy of Jiří Dolejší.)

Refs. [69, 70, 71].

To characterize the process of in-medium parton radiation one needs to introduce following quantities:

- energy of the initial parton, E,
- energy of the emitted gluon, ω,
- transverse momentum of the emitted gluon, k_t,
- transverse momentum exchanged with the medium, q_t,
- spatial extent of the medium (thickness), L.

These quantities are illustrated in the sketch of the medium-induced gluon radiation shown in Fig. 5. To further characterize the interaction it is useful to introduce mean free path λ, opacity $\bar{n}$, and transport coefficient $\hat{q}$. The mean free path is given by a standard relation

$$\lambda = \frac{1}{\sigma\rho}, \tag{19}$$

where σ is an elastic cross-section and ρ is a density of the medium. Opacity or geometrical thickness of the medium,

$$\bar{n} = \frac{L}{\lambda}, \tag{20}$$

is a number of scatterings experienced by the particle in the medium of thickness L. Transport coefficient characterizes the scattering strength of the medium and it is defined as the average transverse momentum squared transferred to the traversing particle per unit path length,

$$\hat{q} = \frac{\langle q_t^2 \rangle}{\lambda}. \tag{21}$$

With these quantities at hand, basic properties of the gluon radiation can be discussed.

The gluon radiation can be described in terms of its transverse momentum, k_t, energy, $\omega = |\vec{k}|$, and the angle between the direction of the gluon and the direction of the parent parton, $\theta \simeq k_t/\omega$. One effect which was found to be important for the in-vacuum radiation of partons is the effect of color coherence. While the gluon emission vertex is local, the emission process is truly non-local. When the gluon starts to get emitted its wave function overlaps with the wave function of the parent parton and the system acts coherently meaning that the two quanta cannot be distinguished from each other (first observation of these kind of coherence effects was done in fifties by Chudakov [72]). This means that it takes some time for the gluon to be fully formed. This time is called "formation time." The gluon can be considered fully formed if the spacial distance between the gluon and the parent parton, $d_\perp \simeq \theta \Delta t$, is larger then its Compton wave-length, $\lambda_\perp = 1/k_t \simeq 1/(\omega\theta)$. This condition implies that the formation time is

$$t_{\rm form} \simeq \frac{2\omega}{k_t^2} \simeq \frac{2}{\omega\theta^2}. \tag{22}$$

Here the factor of two in the numerator is conventional. Equation (22) holds for the radiation in the vacuum as well as for the radiation in the medium. In the case of the vacuum, virtual parton tends to decrease its virtuality by radiating off gluons. The spectrum of these gluons is preferably soft and collinear for which the formation time of gluons is long. In the case of the vacuum, there is no simple relation between k_t and ω (besides the energy momentum conservation) that could be based on some general arguments about the properties of the radiation. On the contrary such arguments can be put forward in the case of the medium.

In the case of the medium, the parton scatters on deconfined scattering centers. The parton acquires a small acceleration at each scattering which leads to radiation of gluons. The initial virtuality is not a driving factor of the radiation in this case. Medium induced gluons accumulate k_t via re-scatterings in the medium during their formation. This implies that k_t, which is due to N scatterings (we assume that the radiated gluon scatters at N scattering centers and that each scattering is independent from another scattering), is related to $\hat{q}$ through the transverse momentum conservation as follows,

$$\hat{q} = \frac{\langle q_t^2 \rangle}{\lambda} = \frac{N \langle q_t^2 \rangle}{N\lambda} = \frac{k_t^2}{t_{\rm form}}. \tag{23}$$

Here we also assumed that the formation time was larger than the mean free path in the medium. Using the previous relation and Eq. (22) for the formation time one can derive following relations,

$$k_t^2 = \sqrt{2\omega\hat{q}}, \tag{24}$$

$$t_{\rm form} = \sqrt{\frac{2\omega}{\hat{q}}}. \tag{25}$$

This tells us that there is a relation between k_t and ω in the case of the in-medium radiation and that the gluon formation time grows with the energy as $t_{\rm form} \propto \sqrt{\omega}$.

In Eq. (23), we assumed that the formation time is larger than the mean free path in the medium and smaller than the size of the medium, i.e.

$$\lambda < t_{\rm form} < L. \tag{26}$$

This implies that the radiated energies are in the interval of ω_{min} and ω_{max} where the later is termed characteristic energy, ω_c, in the literature. Using (25) in the form $\omega = \frac{1}{2}\hat{q}t_{\rm form}$ one can get following relations for ω_{min} and ω_c,

$$\omega_{min} = \frac{1}{2}\hat{q}\lambda^2, \tag{27}$$

$$\omega_c = \frac{1}{2}\hat{q}L^2. \tag{28}$$

Using the relation $\theta \simeq k_t/\omega$ and Eq. (24) one obtains for the angle θ,

$$\theta = \sqrt[4]{\frac{2\hat{q}}{\omega^3}}, \tag{29}$$

which allows to use Eqs. (27),(28) and get estimates for the minimal and maximal angle,

$$\theta_c = \frac{2}{\sqrt{\hat{q}L^3}}, \tag{30}$$

$$\theta_{max} = \frac{2}{\sqrt{\hat{q}\lambda^3}}. \tag{31}$$

The existence of minimal angle, θ_c, and maximal angle is characteristic for the radiation in the medium compared to the radiation in the vacuum. For values of $\hat{q} = 1$ GeV^2/fm and $L = 10$ fm the minimal angle is rather small, approximately 0.01 radian.

The distribution of angles or energies of the radiated quanta in the medium can be generally characterized by the Gunion-Bertsch (GB) spectrum [73],

$$\omega\frac{{\rm d}^2I}{{\rm d}\omega{\rm d}z}\bigg|_{GB} \simeq \frac{\alpha_s}{\lambda} \tag{32}$$

(here I stands for intensity, a dimensionless quantity which is proportional to the number of gluons, and ${\rm d}z$ is a differential over the path-length). If each of N scatterings is independent from another scattering, then the total medium-induced gluon spectrum can be expressed as

$$\omega\frac{{\rm d}^2I}{{\rm d}\omega{\rm d}z} \simeq \frac{1}{N}\omega\frac{{\rm d}^2I}{{\rm d}\omega{\rm d}z}\bigg|_{GB} \simeq \frac{1}{N}\frac{\alpha_s}{\lambda} \simeq \frac{\alpha_s}{t_{\rm form}} \simeq \alpha_s\sqrt{\frac{\hat{q}}{2\omega}} \simeq \alpha_s\sqrt{\frac{\omega_c}{\omega}}. \tag{33}$$

This means that the radiation spectrum is dominated by soft gluons. One can see from Eq. (29) that these soft gluons are radiated at large angles. This basic property that we obtained from very simple arguments is indeed confirmed by experiments as discussed in the previous section.

Finally, we can integrate Eq. (33) from 0 to ω_c, which gives the estimate for a total energy lost by a parton,

$$\langle \Delta E \rangle = \int_0^{\omega_c} \omega \frac{\mathrm{d}^2 I}{\mathrm{d}\omega \mathrm{d}z} \propto \omega_c \propto \hat{q} L^2. \tag{34}$$

This implies that the average radiative energy loss grows quadratically with in-medium path length. This qualitative property together with other properties of the parton energy loss discussed here are recovered in some of detailed theoretical models of the jet quenching.

Above presented calculations are only heuristic. Detailed calculations of the jet quenching, which we will briefly describe now, were done over the last twenty years. The detailed jet quenching calculations can be divided into four classes identified typically by names of their authors:

- BDMPS-Z: Baier, Dokshitzer, Mueller, Piegné, Schiff, and Zacharov [74, 75, 76, 77, 78, 79, 80]; ASW: Armesto, Salgado, Wiedemann [81, 82, 83, 84, 85];
- GLV: Gyulassy, Lévai, Vitev [86, 87, 88, 89];
- HT (Higher Twist): Luo, Qiu, Sterman [90, 91, 92, 93, 94, 95];
- AMY: Arnold, Moore, Yaffe [96, 97, 98, 99, 100].

While these four classes differ in relations between the scales and in assumptions on the structure of the medium, they use assumptions discussed above on the evolution of the gluon radiation. Namely, all schemes assume the collinear approximation, $\omega \gg k_t$, and all schemes except AMY assume the soft radiation approximation, $E \gg \omega$. All schemes are based on the pQCD factorization and calculate the medium induced modifications of the in-vacuum parton showering. The hadronization process is always assumed to take place in the vacuum.

BDMPS/ASW and GLV compute modification of the fragmentation function via the parton radiated gluon spectrum. BDMPS/ASW uses path-integral techniques to calculate the energy loss in the approximation of multiple-soft scatterings. The propagation of the initial parton and radiated gluons is expressed using Green's functions which are obtained by a path integral over the quark and gluon fields and the resulting radiated gluon spectrum is calculated as a function of $\hat{q}$. The radiated gluon spectrum can be then used to calculate so called quenching weights, P_E, that encode the probability that the propagating parton loses a fraction of energy $\epsilon = \Delta E/E$ due to n gluon emissions,

$$P_E(\epsilon, \hat{q}) = \sum_{n=0}^{\infty} \frac{1}{n!} \left[\prod_{i=1}^{n} \int \mathrm{d}\omega_i \frac{\mathrm{d}I^{\mathrm{med}}(\hat{q})}{\mathrm{d}\omega} \right] \delta\left(\epsilon - \sum_{i=1}^{n} \frac{\omega_i}{E} \right) \exp\left[- \int \mathrm{d}\omega \frac{\mathrm{d}I^{\mathrm{med}}(\hat{q})}{\mathrm{d}\omega} \right]. \tag{35}$$

The quenching weight can be then used to calculate modified fragmentation functions,

$$D^{\mathrm{med}}(z_h', \mu^2) = P_E(\epsilon, \hat{q}) \otimes D^{\mathrm{vac}}(z_h, \mu^2), \tag{36}$$

where z_h is the momentum fraction carried by a hadron and μ is the factorization scale. GLV starts with single-hard radiation spectrum and performs a systematic expansion in terms of number of scatterings (opacity expansion). This leads to a probability function similar to (35) which can be then used to calculate modified fragmentation functions as in (36).

HT and AMY compute directly the medium-modified fragmentation functions. HT approach was originally used to describe processes in nuclear deep-inelastic scattering of e+A collisions [90, 91, 92, 93] and di-hadron fragmentation functions in e^+e^- collisions [101, 102]. This work was then followed by applying HT to calculate the parton energy loss in heavy ion collisions [94, 95]. HT assumes finite number of scattering centers and computes medium-modified fragmentation function via the modified splitting functions. Therefore, HT is formally similar to DGLAP formalism. Medium modified fragmentation function for a transition of a parton i into a hadron h can be expressed as $D^{\rm med}_{i\to h} = D^{\rm vac}_{i\to h} + \Delta D^{\rm med}_{i\to h}$, where

$$\Delta D^{\rm med}_{i\to h}(z_h,\mu^2) = \int_0^{\mu^2} \frac{{\rm d}k_t^2}{k_t^2}\frac{\alpha_s}{2\pi}\Big[\int_{z_h}^1 \frac{{\rm d}z}{z}\sum_{j=q,g}\Big(\Delta P^{\rm med}_{i\to j}(z,k_t^2)D_{j\to h}\Big(\frac{z_h}{z},\mu^2\Big)\Big)\Big]. \qquad (37)$$

Here $\Delta P_{i\to j} \simeq P_{i\to j}T^A_{qg}$ is the medium modified splitting function which incorporates the medium modification via the nuclear quark-gluon correlation function T^A_{qg}. The overall normalization of the T^A_{qg}, called correlation constant C, is a free parameter of the theory.

In the AMY scheme, the medium modified fragmentation function is modeled by a convolution of the vacuum fragmentation function with hard parton distributions. The evolution of the hard parton distributions is described by an equation that formally resembles Fokker-Plank equation (Fokker-Plank equation describes the time evolution of probability distribution function describing a position of a particle in stochastic processes, e.g. diffusion or Brownian motion). AMY assumes infinite number of scatterings in the equilibrated medium and on-shell initial partons with energies of the order of the temperature of the medium. The assumption of high temperature allows to use hard-thermal-loop improved pQCD. Free parameters of AMY are the temperature and α_s.

Generally, HT and AMY are very different models, whereas BDMPS/ASW and GLV are similar. Even if all the models have different parameters that control the energy loss, they can be roughly compared in terms of the transport coefficient $\hat{q}$ that can be extracted from the models' fits to the RHIC R_{AA} data. To make the comparison meaningful, differences among models that are not directly related to the implementation of the energy loss mechanism, such as the choice of the time-dependent medium density profiles or initial production spectra, has to be reduced. Even after reducing these differences, the $\hat{q}$ can differ by a factor of ten. For the medium of size $L = 5$ fm, the largest value of $\hat{q}$ is 2 GeV^2/fm [103]. Large differences in the $\hat{q}$ indicate that more work is needed to understand the differences among models and possibly to implement features that are ignored by the models.

One effect that is not considered in the above described models is the impact of the medium on the color-coherence of the parton shower. Studies of this effect [104, 105, 106, 107] suggest that the medium is actually unable to resolve the internal structure of many jets. Those jets then interact with the medium as if they consist of a single color charge, and the reduced-energy jet fragments as if it was in the vacuum. The phenomenological impact of these ideas/results along with analysis of unexpected features seen in the fragmentation function measurement in Pb+Pb collisions at the LHC is provided in Ref. [23] included in Section 6.4. If the parton shower, or its large part, radiates as one object, one can ask if it is possible to find some similarities between the suppression of jets and a suppression of other objects with an internal structure observed in heavy ion collisions. A search for such similarity is described in Ref. [24] included in Section 6.4.

Understanding the color coherence effects and the similarity between the jet quenching and other suppression phenomena such as quarkonia suppression should improve our knowledge about the fundamental process of particle radiation as well as about the process of hadron formation. In a wider context, it should also help us to understand the properties of the strongly interacting matter created in heavy ion collisions as briefly summarized in Section 5.

4 Overview of ATLAS heavy ion physics program

This section summarizes the ATLAS heavy ion physics program from the LHC run 1 which took place between 2010 and 2013. It aims to put the jet measurements into the context of other measurements performed within ATLAS heavy ion working group. The text of this section is largely based on the overview proceedings paper associated with my plenary talk at Hard Probes International Conference in 2015 which was published in Ref. [108].

4.1 Heavy ion runs at the LHC

The LHC heavy ion physics program started in fall 2010. During that period ATLAS collected 7 μb^{-1} of Pb+Pb collisions at $\sqrt{s_{\text{NN}}} = 2.76$ TeV. In fall 2011, ATLAS collected 0.14 nb^{-1} of Pb+Pb data at $\sqrt{s_{\text{NN}}} = 2.76$ TeV. In fall 2012 a pilot proton-lead (p+Pb) run was realized delivering approximately 1 μb^{-1} of collisions at $\sqrt{s_{\text{NN}}}$= 5.02 TeV. The full p+Pb run at the same center-of-mass energy followed in the winter 2013 delivering approximately 28 nb^{-1}. Some of the measurements done with Pb+Pb collisions use as a reference pp collisions delivered at the same center-of-mass energy, that is $\sqrt{s} = 2.76$ TeV, which were provided by the LHC in the year 2013. These pp collisions together with pp collisions at 7 or 8 TeV are used also to construct a reference at 5.02 TeV which is used in some of the p+Pb measurements. The results from p+Pb collisions are summarized in Section 4.2, the results from Pb+Pb collisions are summarized in Section 4.3.

In spring 2015, a new period of runs at the LHC began, called run 2. During that period protons were collided at the centre-of-mass energy of 13 TeV, which is close to the design value of 14 TeV. In fall 2015, Pb+Pb collisions and pp collisions at the center-of-mass energy of 5 TeV were provided by the LHC. These data are currently analyzed and only first few preliminary results were published which are not included in this overview.

4.2 Physics of p+Pb collisions

Prior to the first LHC runs of p+Pb collisions, the main motivation for running these collisions was to improve the understanding of the initial state effects of nuclear collisions, namely to quantify the modifications of parton distribution functions in the nuclear environment. The studies done with p+Pb data were primarily intended to be a reference for studies of processes in Pb+Pb collisions, where a deconfined matter is produced. However, the p+Pb collisions have brought several unexpected observations, such as double-ridge structure in long range pseudorapidity correlations, significant centrality and rapidity dependence of the inclusive jet production, and an enhancement of charged particle yields. In this section we summarize the run 1 studies of p+Pb collisions provided by ATLAS starting from measurements of jet yields, going through measurements of correlations between soft and hard processes, Z boson, J/ψ and $\psi(2)$ production, jet fragmentation, and closing by studies of the azimuthal correlations in p+Pb collisions.

Measurement of the inclusive jet production in p+Pb [109] was expected to provide a valuable benchmark for the jet quenching measured in Pb+Pb collisions. Indeed, a good correspondence of the jet spectra measured inclusively in centrality with the pQCD prediction employing the EPS09 parameterization of nuclear parton distribution functions (nPDF) [110] was seen, which confirms that the jet suppression seen in Pb+Pb collisions is due to

final state effects. The nuclear modification factor of inclusive jets, $R_{p\mathrm{Pb}}$, exhibits only little (if any) deviation from unity. On the contrary, the ratios of inclusive jet spectra from different centrality selections show a strong modification of jet production at all p_T at forward rapidities and for large p_T at mid-rapidity, which manifests as a suppression of the jet yield in central events and an enhancement in peripheral events. These effects imply that the factorization between hard and soft processes is violated at an unexpected level in proton-nucleus collisions. Furthermore, the modifications at forward rapidities were found to be a function of the total jet energy only, implying that the violations might have a simple dependence on the hard parton-parton kinematics.

To improve the understanding of soft-hard correlations ATLAS measured the relationship between jet production and the underlying event in a pseudorapidity separated region in 2.76 TeV pp collisions [111]. In that study, the underlying event was characterized through measurements of the average sum of the transverse energy at large negative pseudorapidity, $\langle \Sigma E_{\mathrm{T}} \rangle$, which were reported as a function of hard scattering kinematic variables. The hard scattering was characterized by the average transverse momentum, p_T^{avg}, and pseudorapidity, η^{avg}, of the two highest transverse momentum jets in the event. It was found that the $\langle \Sigma E_{\mathrm{T}} \rangle$ is anticorrelated with the dijet p_T^{avg}, decreasing by 25% as p_T^{avg} varies from 50 to 500 GeV. This general trend is reproduced by leading-order Monte Carlo (MC) generators. These anticorrelations measured in pp collisions provide a useful context for understanding the p+Pb results, since they indicate a nontrivial correlation between hard scattering kinematics and ΣE_{T} production.

Further insight was gained by estimating, from the dijet kinematics on an event-by-event basis, the scaled longitudinal momenta of the hard scattered partons in protons. This was done separately in the projectile and target beam-protons defined as moving to positive and negative rapidity, respectively. Transverse energy production at large negative pseudorapidity was observed to be linearly dependent on the longitudinal momentum fraction in the target proton, x_{targ}, and only weakly with that in the projectile proton, x_{proj}. This shows that the average level of transverse energy production is sensitive predominantly to the Bjorken-x of the parton originating in the beam-proton which is headed towards the energy-measuring region (x_{targ}), and is mostly insensitive to x in the other proton (x_{proj}).

These results provide counter-evidence to claims that a simple anti-correlation between soft transverse energy production at negative pseudorapidity and dijet hard-scattering kinematics at positive rapidity in individual nucleon-nucleon collisions can trivially explain the observed modification of the forward, or proton-going, jet rate in centrality selected p+Pb collisions (simple anti-correlation being due to e.g. energy conservation – see Ref. [112]). In the p+Pb data, the deviations from the expected centrality dependence are observed to depend only on, and increase with, x in the proton, that is with x_{proj}. Therefore, for this effect to be consistent with arising from such a simple anti-correlation, transverse energy production at small angles should decrease strongly and continuously with increasing x_{proj}.

Better understanding of the interplay between soft and hard physics and centrality in p+Pb can be gained also from the measurement of Z boson production [113]. An important component of the measurement is the centrality bias correction [114] which should reduce the correlation between hard process rates and the magnitude of the soft event activity. After applying the centrality bias correction the N_{coll} scaled yield of Z bosons is approximately centrality independent, consistent with a production mechanism that scales with the number

of binary collisions – though this scaling is less good for Glauber-Gribov Colour Fluctuation model [115, 116] than for the simple Glauber model. The Z boson production cross section measured as a function of rapidity and x_{Pb} is systematically larger compared to predictions based on perturbative QCD calculations even after including effects from modifications of nPDF as predicted by EPS09.

While the next-to-leading order (NLO) pQCD with EPS09 does not fully describe the rapidity dependence of the Z boson production, it was found to describe well the rapidity dependence of the prompt J/ψ production, measured over p_T interval of $8-30$ GeV [117]. In that measurement, the non-prompt and prompt J/ψ production cross-section was evaluated as a function of p_T and rapidity. Also measured was the $\psi(2)$ [118]. The non-prompt J/ψ and $\psi(2)$ cross-sections were found to be described, though with large theoretical uncertainties, by FONLL calculations [119] which do not include nuclear effects. Further, the nuclear modification factor, $R_{p\mathrm{Pb}}$, was evaluated based on an interpolation of the cross sections at 2.76, 7 and 8 TeV. The $R_{p\mathrm{Pb}}$ of both prompt and non-prompt J/ψ were measured to be not more than $10-30\%$ above unity showing no significant dependence on p_T and rapidity. After applying the centrality bias correction, the $R_{p\mathrm{Pb}}$'s do not exhibit dependence on number of participating nucleons. The centrality bias correction also weakens the linear correlation between the self-normalized ratios of J/ψ, $\psi(2)$, and Z boson production and self-normalized transverse energy measured in the forward calorimeter, $E_{\mathrm{T}}^{\mathrm{FCal}}/\langle E_{\mathrm{T}}^{\mathrm{FCal}}\rangle$.

While the $R_{p\mathrm{Pb}}$ of J/ψ shows a possible modest enhancement with no significant p_T dependence, the previously measured charged particle $R_{p\mathrm{Pb}}$ exhibited a significant increase for $p_T \gtrsim 10-20$ GeV reaching a maximum of 1.4 at $p_T \approx 60$ GeV [120]. This unexpected excess in yields of charged particles seen across different rapidity bins contrasts with only little modification seen in the measurement of inclusive jet production discussed previously. Thus, a measurement of jet fragmentation was performed [121] to shed light on the origin of this effect. In that measurement, the p+Pb data were compared to a pp reference, constructed by extrapolating the measured fragmentation functions in 2.76 TeV pp collisions to 5.02 TeV. Using this reference, a ratio of fragmentation functions, $R_{D(z)} = D(z)|_{p\mathrm{Pb}}/D(z)|_{pp}$, was constructed. The measured $R_{D(z)}$ exhibits a z-dependent excess with a maximal magnitude of approximately 10% for $0.2 \lesssim z \lesssim 0.8$ in jets with $p_T > 80$ GeV. The z and p_T ranges over which the $R_{D(z)}$ distributions are enhanced correspond to the same range in transverse momentum where the inclusive charged particle spectrum in p+Pb collisions is enhanced.

Not only high-p_T probes measured in p+Pb collisions brought new interesting physics, but also a region of low p_T revealed unexpected strong signals. Shortly after the first p+Pb run a double-ridge structure in long-range pseudorapidity correlations was observed in high-multiplicity p+Pb collisions [122]. In subsequent studies [123, 124], the azimuthal structure of such long-range correlations was Fourier decomposed to obtain the harmonics v_n as a function of p_T and event activity. The extracted v_n values for $n = 2$ to 5 decrease with n. The v_2 and v_3 values were found to be positive in the measured p_T range. The v_1 was also measured as a function of p_T and was observed to change sign around $p_T \approx 1.5-2$ GeV and then increase to about 0.1 for $p_T > 4$ GeV. The $v_2(p_T)$, $v_3(p_T)$ and $v_4(p_T)$ were compared to the v_n coefficients in Pb+Pb collisions at $\sqrt{s_{\mathrm{NN}}} = 2.76$ TeV with similar event multiplicities. Reasonable agreement was observed after accounting for the difference in the average p_T of particles produced in the two collision systems. This agreement suggests that the long-range ridge correlations in high-multiplicity p+Pb collisions and peripheral Pb+Pb collisions are

driven by similar dynamics.

4.3 Physics of Pb+Pb collisions

Not only p+Pb collisions but also measurements of high-p_T photons and electroweak bosons in Pb+Pb collisions can be used to study the nuclear initial state effects and the role of the geometry of colliding nuclei. Recently, the prompt photon production [125] and the production of $W^{\pm}$ [126] was measured in Pb+Pb collisions. Earlier, the production of Z bosons in Pb+Pb collisions was studied [127].

Inclusive photon yields, scaled by the mean nuclear thickness function, were measured as a function of collision centrality and transverse momentum in two pseudorapidity intervals, $|\eta| < 1.37$ and $1.52 \leq |\eta| < 2.37$. The scaled yields in the two pseudorapidity intervals, as well as the ratios of the forward yields to those at midrapidity, were compared to the expectations from next-to-leading order perturbative QCD calculations from Jetphox [128]. The scaled yields agree well with the predictions for pp collisions within statistical and systematic uncertainties. Both the yields and ratios of prompt photons were also compared to two other pQCD calculations, one which uses the isospin content appropriate to colliding lead nuclei and another which includes the EPS09 nuclear modifications to the nucleon parton distribution functions. The data are unable to distinguish between the three scenarios. However, the overall consistency of the measured yields with Jetphox expectations for all centrality intervals demonstrates that photon yields in heavy ion collisions scale with $N_{\rm coll}$, that is with the mean nuclear thickness, as expected.

The $W^{\pm}$ boson production was measured in electron and muon decay channels. The differential production yields and lepton charge asymmetry were each measured as a function of the average number of participating nucleons $\langle N_{\rm part} \rangle$ and absolute pseudorapidity of the charged lepton, $|\eta_l|$, within $|\eta_l| < 2.5$. The W boson yields scaled by $1/\langle N_{\rm coll} \rangle$ were found to be independent of centrality and in a good agreement with NLO pQCD predictions. Due to the different isospin content of Pb+Pb compared to pp collisions, the lepton charge asymmetry from $W^{\pm}$ boson decays differs from that measured in pp collisions. The lepton charge asymmetry agrees well with theoretical predictions using pQCD at NLO with CT10 [129] PDF sets with and without EPS09 nuclear corrections. Clearly, further improvements in the experimental precision and uncertainties in the theory are needed to establish the existence of nuclear effects. Despite that, these measurements provide further support for the interpretation of the clear modification of jet yields in Pb+Pb collisions as a function of centrality, relative to those measured in proton-proton collisions, as stemming from energy loss in the hot, dense medium.

First measurement of jet suppression [16, 17] were followed by a precise measurement of jet nuclear modification factor, $R_{\rm AA}$, which was evaluated as a function of centrality, jet p_T, and jet rapidity [18] and which was discussed in Section 3.2. The jet $R_{\rm AA}$ was found to reach a value of approximately 0.5, implying that the jet yields are suppressed by a factor of two in central collisions compared to pp collisions. The $R_{\rm AA}$ shows a slight increase with p_T and no significant variation with rapidity. A complementary measurement to the jet $R_{\rm AA}$ is the $R_{\rm AA}$ of charged particles [62]. In that analysis, the charged particle spectra were measured over a wide transverse momentum range, $0.5 < p_T < 150$ GeV, and in eight bins in pseudorapidity covering the range of $|\eta| < 2$. The charged particle $R_{\rm AA}$'s show a distinct p_T dependence with

a pronounced minimum at about 7 GeV. Above 60 GeV, $R_{\rm AA}$ is consistent with a plateau at a centrality-dependent value which is approximately 0.55 for the 0–5% most central collisions. The $R_{\rm AA}$ distribution is consistent with flat pseudorapidity dependence over the whole transverse momentum range in all centrality classes. Our understanding of the jet quenching should also strongly profit from the direct measurement of jet fragmentation [19] discussed in Section 3.2. In that measurement, it was found that the central-to-peripheral ratios of fragmentation functions of jets with $p_T > 100$ GeV show a reduction of fragment yield in central collisions relative to peripheral collisions at intermediate z values, $0.04 < z < 0.2$ and an enhancement in fragment yield for $z < 0.04$. A smaller, less significant enhancement was observed at large z in central collisions. Similar observations were done also for the distributions of transverse momenta of charged particles reconstructed inside jets.

To improve understanding of the path length dependence of the jet quenching and the role of fluctuations in the jet quenching, three more differential measurements have been performed: the measurement of azimuthal dependence of inclusive jet yields [64] and more recently the measurement of correlation between dijet-asymmetry and event-shape variables [65] and the measurement of neighbouring jet production [20]. These measurements were discussed in Section 3.2. The main result of these measurement is an observation of weak c_2 signal in the dijet asymmetry, significant single jet v_2 and a presence of characteristic increase in the neighbouring jet yields when evaluated as a function of neighbouring jet E_T. At high-transverse momenta, the azimuthal angle anisotropy characterized by v_2 and c_2 is understood to result from the path-length dependent energy loss of jets as they traverse the deconfined matter. At low transverse momenta ($p_T \lesssim 3-4$ GeV), this anisotropy results from a pressure driven anisotropic expansion of the created matter, with more particles emitted in the direction of the largest pressure gradient. This is commonly called (elliptic) flow phenomenon which is successfully described by calculations based in relativistic hydrodynamics [130, 131]. In Pb+Pb collisions, ATLAS has performed event-averaged measurement of elliptic flow and higher order flow harmonics [132, 133, 134, 135], the event-by-event flow measurements [136] and the measurement of event plane correlations [137]. Recently, ATLAS has performed also the measurement of correlations between different flow harmonics in Pb+Pb collisions [138]. In that measurement, it was found that v_3 is anticorrelated with v_2 and this anticorrelation is consistent with similar anticorrelations between the corresponding eccentricities ϵ_2 and ϵ_3. On the other hand, it was observed that v_4 increases strongly with v_2, and v_5 increases strongly with both v_2 and v_3. The trend and strength of the $v_m - v_n$ correlations for $n = 4$ and 5 were found to disagree with $m - n$ correlations predicted by initial-geometry models. Instead, these correlations were found to be consistent with the combined effects of a linear contribution to v_n and a nonlinear contribution that is a function of v_2 or of $v_2 v_3$, as predicted by hydrodynamic models.

A complementary measurement to the measurement of correlations of azimuthal harmonics is the measurement of two particle pseudorapidity correlations [139]. Two particle pseudorapidity correlations can probe e.g. the rapidity profile of the initial-state fireball. This ATLAS measurement was done in the pseudorapidity range of $|\eta| < 2.4$ with charged particles having $p_T > 0.5$ GeV. The measured two particle correlation functions show a broad "ridge-like" shape along $\eta_1 = \eta_2$ and a depletion at around $\eta_1 = -\eta_2$. The correlation functions were expressed in terms of $\eta_- \equiv \eta_1 - \eta_2$ and $\eta_+ \equiv \eta_1 + \eta_2$ which allows to separate the short-range correlation effects (centered around $\eta_- \approx 0$) from the genuine long-range

correlations. Further, the measured two particle correlation functions were expanded in terms of products of Legendre polynomials, $T_n(\eta_1)T_m(\eta_2)$, and corresponding coefficients, $a_{n,m}$, were extracted. The first term, $\sqrt{\langle a_n^2 \rangle}$, is connected with the asymmetry between forward and backward particle production which was confirmed to be large as seen previously in other measurements. The second term reflects the even-by-event fluctuation of the width of charged particle multiplicities, $N(\eta)$. Significant mixed coefficients $\langle a_n, a_m \rangle$ are also observed. The most significant group of mixed coefficients $\langle a_n, a_{n+2} \rangle$ is found to be negative, implying that a_n and a_{n+2} are generally anticorrelated. The magnitudes of $\langle a_n, a_{n+2} \rangle$, were found to decrease quickly for larger n. These extracted coefficients are generally found to increase for peripheral collisions, which is consistent with the increase of the multiplicity fluctuation for smaller collision systems.

The correlation measurements discussed in this section should help to better understand the (fluctuating) initial conditions of expanding medium and to further test the hydrodynamical paradigm. Wealth of experimental results by ATLAS from LHC run 1 should be followed by new measurements in the run 2 which is planned for years $2015 - 2018$.

5 Summary and outlook

First sections of this habilitation thesis aimed to provide a motivation and context for publications included in the next section. A common theme of these publications is a study of jets in pp collisions and mainly in heavy-ion collisions: experimental measurements of jets and their properties, technical background needed for jet measurements, and a phenomenological interpretation of some aspects of jet measurements related to jet quenching.

Wealth of experimental results by ATLAS from LHC run 1 should be followed by new measurements in the run 2 which is planned for years $2015-2018$ and precise measurements in run $3-5$ which are planned for years $2021-2033$. Studies that will use new high-statistics data should bring a better understanding of the jet quenching, flow, charmonia suppression, nuclear initial state, correlations between soft and hard particle production, ultra-peripheral heavy ion collisions, and other interesting phenomena. These are individual bricks that should ultimately help to build new bridges: a bridge between the perturbative description of the strong interaction and the non-perturbative world of hadronization; a bridge between understanding the evolution of the deconfined medium created in the laboratory and the evolution of matter during the cool-down of the universe; a bridge between the use of advanced mathematical tools such as the AdS/CFT correspondence and the description of real phenomena present in the nature. Besides these goals, the jet quenching itself should help to understand general aspects of the process of radiation: formation of radiated quanta, role of coherence effects in the radiation, magnitude of scales relevant in the radiation process. I believe that these questions and answers to them will continue to excite and attract people and that it will bring a new fundamental knowledge.

References

[1] Glashow S.L., *Partial Symmetries of Weak Interactions*, Nucl. Phys. **22** (1961), 579–588, doi: 10.1016/0029-5582(61)90469-2

[2] Weinberg S., *A Model of Leptons*, Phys. Rev. Lett. **19** (1967), 1264–1266, doi: 10.1103/PhysRevLett.19.1264

[3] Salam A., *Weak and Electromagnetic Interactions*, Conf. Proc. **C680519** (1968), 367–377

[4] 't Hooft G. and Veltman M.J.G., *Regularization and Renormalization of Gauge Fields*, Nucl. Phys. **B44** (1972), 189–213, doi: 10.1016/0550-3213(72)90279-9

[5] Englert F. and Brout R., *Broken Symmetry and the Mass of Gauge Vector Mesons*, Phys. Rev. Lett. **13** (1964), 321–323, doi: 10.1103/PhysRevLett.13.321

[6] Higgs P.W., *Broken symmetries, massless particles and gauge fields*, Phys. Lett. **12** (1964), 132–133, doi: 10.1016/0031-9163(64)91136-9

[7] Higgs P.W., *Broken Symmetries and the Masses of Gauge Bosons*, Phys. Rev. Lett. **13** (1964), 508–509, doi: 10.1103/PhysRevLett.13.508

[8] Guralnik G.S., Hagen C.R., and Kibble T.W.B., *Global Conservation Laws and Massless Particles*, Phys. Rev. Lett. **13** (1964), 585–587, doi: 10.1103/PhysRevLett.13.585

[9] Higgs P.W., *Spontaneous Symmetry Breakdown without Massless Bosons*, Phys. Rev. **145** (1966), 1156–1163, doi: 10.1103/PhysRev.145.1156

[10] Kibble T.W.B., *Symmetry breaking in nonAbelian gauge theories*, Phys. Rev. **155** (1967), 1554–1561, doi: 10.1103/PhysRev.155.1554

[11] Aad G. et al., *Observation of a new particle in the search for the Standard Model Higgs boson with the ATLAS detector at the LHC*, Phys. Lett. **B716** (2012), 1–29, doi: 10.1016/j.physletb.2012.08.020

[12] Chatrchyan S. et al., *Observation of a new boson at a mass of 125 GeV with the CMS experiment at the LHC*, Phys. Lett. **B716** (2012), 30–61, doi: 10.1016/j.physletb.2012.08.021

[13] Aad G. et al., *Combined Measurement of the Higgs Boson Mass in pp Collisions at $\sqrt{s} = 7$ and 8 TeV with the ATLAS and CMS Experiments*, Phys. Rev. Lett. **114** (2015), 191803, doi: 10.1103/PhysRevLett.114.191803

[14] Aad G. et al., *Measurement of inclusive jet and dijet cross sections in proton-proton collisions at 7 TeV centre-of-mass energy with the ATLAS detector*, Eur. Phys. J. **C71** (2011), 1512, doi: 10.1140/epjc/s10052-010-1512-2

[15] Aad G. et al., *Study of Jet Shapes in Inclusive Jet Production in pp Collisions at $\sqrt{s} = 7$ TeV using the ATLAS Detector*, Phys. Rev. **D83** (2011), 052003, doi: 10.1103/PhysRevD.83.052003

[16] Aad G. et al., *Observation of a Centrality-Dependent Dijet Asymmetry in Lead-Lead Collisions at $\sqrt{s_{NN}} = 2.77$ TeV with the ATLAS Detector at the LHC*, Phys. Rev. Lett. **105** (2010), 252303, doi: 10.1103/PhysRevLett.105.252303

[17] Aad G. et al., *Measurement of the jet radius and transverse momentum dependence of inclusive jet suppression in lead-lead collisions at $\sqrt{s_{NN}}$= 2.76 TeV with the ATLAS detector*, Phys. Lett. **B719** (2013), 220–241, doi: 10.1016/j.physletb.2013.01.024

[18] Aad G. et al., *Measurements of the Nuclear Modification Factor for Jets in Pb+Pb Collisions at $\sqrt{s_{\mathrm{NN}}} = 2.76$ TeV with the ATLAS Detector*, Phys. Rev. Lett. **114** (2015), 072302, doi: 10.1103/PhysRevLett.114.072302

[19] Aad G. et al., *Measurement of inclusive jet charged-particle fragmentation functions in Pb+Pb collisions at $\sqrt{s_{NN}} = 2.76$ TeV with the ATLAS detector*, Phys. Lett. **B739** (2014), 320–342, doi: 10.1016/j.physletb.2014.10.065

[20] Aad G. et al., *Measurement of the production of neighbouring jets in lead-lead collisions at $\sqrt{s_{\mathrm{NN}}} = 2.76$ TeV with the ATLAS detector*, Phys. Lett. **B751** (2015), 376–395, doi: 10.1016/j.physletb.2015.10.059

[21] Aad G. et al., *The performance of the jet trigger for the ATLAS detector during 2011 data taking*, Eur. Phys. J. **C76** (2016), 526, doi: 10.1140/epjc/s10052-016-4325-0

[22] Berta P., Spousta M., Miller D.W., and Leitner R., *Particle-level pileup subtraction for jets and jet shapes*, JHEP **1406** (2014), 092, doi: 10.1007/JHEP06(2014)092

[23] Spousta M. and Cole B., *Interpreting single jet measurements in Pb + Pb collisions at the LHC*, Eur. Phys. J. **C76** (2016), 50, doi: 10.1140/epjc/s10052-016-3896-0

[24] Spousta M., *On similarity of jet quenching and charmonia suppression*, Phys. Lett. **B767** (2017), 10–15, doi: 10.1016/j.physletb.2017.01.041

[25] Chyla J., PRA-HEP-04-01 (2004), 'Quarks, partons and Quantum Chromodynamics'

[26] Ellis R.K., Stirling W.J., and Webber B.R., Camb. Monogr. Part. Phys. Nucl. Phys. Cosmol. **8** (1996), 1–435, 'QCD and collider physics'

[27] Dokshitzer Y.L., Khoze V.A., Mueller A.H., and Troian S.I., Gif-sur-Yvette, France: Ed. Frontieres (1991) 274 p. (1991), 'Basics of perturbative QCD'

[28] Field R.D., Front. Phys. **77** (1989), 1–366, 'Applications of Perturbative QCD'

[29] Greiner W., Schramm S., and Stein E., Berlin, Germany: Springer (2002) 551 p (2002), 'Quantum chromodynamics'

[30] Patrignani C. et al., *Review of Particle Physics*, Chin. Phys. **C40** (2016), 100001, doi: 10.1088/1674-1137/40/10/100001

[31] Catani S., Dokshitzer Y.L., Seymour M.H., and Webber B.R., *Longitudinally invariant K_t clustering algorithms for hadron hadron collisions*, Nucl. Phys. **B406** (1993), 187–224, doi: 10.1016/0550-3213(93)90166-M

[32] Ellis S.D. and Soper D.E., *Successive combination jet algorithm for hadron collisions*, Phys. Rev. **D48** (1993), 3160–3166, doi: 10.1103/PhysRevD.48.3160

[33] Dokshitzer Y.L., Leder G.D., Moretti S., and Webber B.R., *Better jet clustering algorithms*, JHEP **08** (1997), 001, doi: 10.1088/1126-6708/1997/08/001

[34] Wobisch M. and Wengler T., in *Monte Carlo generators for HERA physics. Proceedings, Workshop, Hamburg, Germany, 1998-1999*, pages 270–279, 1998

[35] Cacciari M., Salam G.P., and Soyez G., *The Anti-k(t) jet clustering algorithm*, JHEP **04** (2008), 063, doi: 10.1088/1126-6708/2008/04/063

[36] Spousta M., *Jet Quenching at LHC*, Mod. Phys. Lett. **A28** (2013), 1330017, doi: 10.1142/S0217732313300176

[37] Miller M.L., Reygers K., Sanders S.J., and Steinberg P., *Glauber modeling in high energy nuclear collisions*, Ann.Rev.Nucl.Part.Sci. **57** (2007), 205–243, doi: 10.1146/annurev.nucl.57.090506.123020

[38] Alver B., Baker M., Loizides C., and Steinberg P., *The PHOBOS Glauber Monte Carlo*, arXiv:0805.4411

[39] Loizides C., Nagle J., and Steinberg P., *Improved version of the PHOBOS Glauber Monte Carlo*, SoftwareX **1-2** (2015), 13–18, doi: 10.1016/j.softx.2015.05.001

[40] Bjorken J.D., *Energy Loss of Energetic Partons in Quark - Gluon Plasma: Possible Extinction of High p(t) Jets in Hadron - Hadron Collisions*, FERMILAB-PUB-82-059-THY (1982)

[41] Arsene I. et al., *Quark gluon plasma and color glass condensate at RHIC? The Perspective from the BRAHMS experiment*, Nucl. Phys. **A757** (2005), 1–27, doi: 10.1016/j.nuclphysa.2005.02.130

[42] Back B.B. et al., *The PHOBOS perspective on discoveries at RHIC*, Nucl. Phys. **A757** (2005), 28–101, doi: 10.1016/j.nuclphysa.2005.03.084

[43] Adams J. et al., *Experimental and theoretical challenges in the search for the quark gluon plasma: The STAR Collaboration's critical assessment of the evidence from RHIC collisions*, Nucl. Phys. **A757** (2005), 102–183, doi: 10.1016/j.nuclphysa.2005.03.085

[44] Adcox K. et al., *Formation of dense partonic matter in relativistic nucleus-nucleus collisions at RHIC: Experimental evaluation by the PHENIX collaboration*, Nucl. Phys. **A757** (2005), 184–283, doi: 10.1016/j.nuclphysa.2005.03.086

[45] Adcox K. et al., *Suppression of hadrons with large transverse momentum in central Au+Au collisions at* $\sqrt{s_{NN}}$ *= 130-GeV*, Phys. Rev. Lett. **88** (2002), 022301, doi: 10.1103/PhysRevLett.88.022301

[46] Adler S.S. et al., *Absence of suppression in particle production at large transverse momentum in* $\sqrt{s_{NN}} = 200$ *GeV d+Au collisions*, Phys. Rev. Lett. **91** (2003), 072303, doi: 10.1103/PhysRevLett.91.072303

[47] Adams J. et al., *Evidence from d + Au measurements for final state suppression of high p(T) hadrons in Au+Au collisions at RHIC*, Phys. Rev. Lett. **91** (2003), 072304, doi: 10.1103/PhysRevLett.91.072304

[48] Cronin J.W. et al., *Production of hadrons with large transverse momentum at 200, 300, and 400 GeV*, Phys. Rev. **D11** (1975), 3105–3123, doi: 10.1103/PhysRevD.11.3105

[49] Frankfurt L.L. and Strikman M.I., *Hard Nuclear Processes and Microscopic Nuclear Structure*, Phys. Rept. **160** (1988), 235–427, doi: 10.1016/0370-1573(88)90179-2

[50] Arneodo M., *Nuclear effects in structure functions*, Phys. Rept. **240** (1994), 301–393, doi: 10.1016/0370-1573(94)90048-5

[51] Kusina A., Lyonnet F., Olness F.I., and Schienbein I., *Frontiers of QCD with Precision nPDFs*, EPJ Web Conf. **112** (2016), 03006, doi: 10.1051/epjconf/201611203006

[52] Adler S.S. et al., *Centrality dependence of direct photon production in s(NN)**(1/ 2) = 200-GeV Au + Au collisions*, Phys. Rev. Lett. **94** (2005), 232301, doi: 10.1103/PhysRevLett.94.232301

[53] Adare A. et al., *Dihadron azimuthal correlations in Au+Au collisions at s(NN)**(1/2) = 200-GeV*, Phys. Rev. **C78** (2008), 014901, doi: 10.1103/PhysRevC.78.014901

[54] Adamczyk L. et al., *Di-Jet Imbalance Measurements at* $\sqrt{s_{NN}} = 200$ *GeV at STAR*, arXiv:1609.03878 (2016)

[55] Aad G. et al., *Measurement of dijet* p_{T} *correlations in Pb+Pb and pp collisions at* $\sqrt{s_{\mathrm{NN}}} = 2.76$ *TeV with the ATLAS detector*, ATLAS-CONF-2015-052 (2015)

[56] Hocker A. and Kartvelishvili V., *SVD approach to data unfolding*, Nucl. Instrum. Meth. **A372** (1996), 469–481, doi: 10.1016/0168-9002(95)01478-0

[57] Aad G. et al., *Internal structure of jets measured in Pb+Pb and pp collisions with the ATLAS detector at the LHC*, ATLAS-CONF-2015-055 (2015)

[58] CMS Collaboration, *Measurement of jet fragmentation in PbPb and pp collisions at* $\sqrt{s_{NN}} = 2.76$ *TeV*, Phys.Rev. **C90** (2014), 024908, doi: 10.1103/PhysRevC.90.024908

[59] CMS Collaboration, *Observation and studies of jet quenching in PbPb collisions at nucleon-nucleon center-of-mass energy = 2.76 TeV*, Phys. Rev. **C84** (2011), 024906, doi: 10.1103/PhysRevC.84.024906

[60] Aad G. et al., *Jet energy scale and its uncertainty for jets reconstructed using the ATLAS heavy ion jet algorithm*, ATLAS-CONF-2015-016 (2015)

[61] Lokhtin I.P. and Snigirev A.M., *A Model of jet quenching in ultrarelativistic heavy ion collisions and high-p(T) hadron spectra at RHIC*, Eur. Phys. J. **C45** (2006), 211–217, doi: 10.1140/epjc/s2005-02426-3

[62] Aad G. et al., *Measurement of charged-particle spectra in Pb+Pb collisions at* $\sqrt{s_{\rm NN}} = 2.76$ *TeV with the ATLAS detector at the LHC*, JHEP **09** (2015), 050, doi: 10.1007/JHEP09(2015)050

[63] Aad G. et al., 2017, arXiv:1702.00674

[64] Aad G. et al., *Measurement of the Azimuthal Angle Dependence of Inclusive Jet Yields in Pb+Pb Collisions at* $\sqrt{s_{NN}} = 2.76$ *TeV with the ATLAS detector*, Phys. Rev. Lett. **111** (2013), 152301, doi: 10.1103/PhysRevLett.111.152301

[65] Aad G. et al., *Measurement of correlations between dijet-asymmetry and event-shape variables in Pb+Pb collisions at* $\sqrt{s_{\rm NN}}$*=2.76 TeV with the ATLAS detector at the LHC*, ATLAS-CONF-2015-021 (2015)

[66] Poskanzer A.M. and Voloshin S.A., *Methods for analyzing anisotropic flow in relativistic nuclear collisions*, Phys. Rev. **C58** (1998), 1671–1678, doi: 10.1103/PhysRevC.58.1671

[67] Abazov V.M. et al., *Measurement of angular correlations of jets at* $\sqrt{s} = 1.96$ *TeV and determination of the strong coupling at high momentum transfers*, Phys. Lett. **B718** (2012), 56–63, doi: 10.1016/j.physletb.2012.10.003

[68] Mustafa M.G., *Energy loss of charm quarks in the quark-gluon plasma: Collisional versus radiative*, Phys. Rev. **C72** (2005), 014905, doi: 10.1103/PhysRevC.72.014905

[69] Wiedemann U.A., *Jet Quenching in Heavy Ion Collisions* (2010), 521–562, doi: 10.1007/978-3-642-01539-7_17, [Landolt-Bornstein23,521(2010)]

[70] Iancu E., *QCD in heavy ion collisions*, in *Proceedings, 2011 European School of High-Energy Physics (ESHEP 2011): Cheile Gradistei, Romania, September 7-20, 2011*, pages 197–266, 2014, doi: 10.5170/CERN-2014-003.197

[71] Baier R., *Jet quenching*, Nucl. Phys. **A715** (2003), 209–218, doi: 10.1016/S0375-9474(02)01429-X

[72] Chudakov A.E., Izv. Akad. Nauk SSSR, Ser. Fiz. **19** (1955), 650, [Bull. Acad. Sci. USSR, Phys. Ser. 19, 589 (1955)]

[73] Gunion J.F. and Bertsch G., *HADRONIZATION BY COLOR BREMSSTRAHLUNG*, Phys. Rev. **D25** (1982), 746, doi: 10.1103/PhysRevD.25.746

[74] Baier R., Dokshitzer Y.L., Peigne S., and Schiff D., *Induced gluon radiation in a QCD medium*, Phys. Lett. **B345** (1995), 277–286, doi: 10.1016/0370-2693(94)01617-L

[75] Baier R., Dokshitzer Y.L., Mueller A.H., Peigne S., and Schiff D., *The Landau-Pomeranchuk-Migdal effect in QED*, Nucl. Phys. **B478** (1996), 577–597, doi: 10.1016/0550-3213(96)00426-9

[76] Baier R., Dokshitzer Y.L., Mueller A.H., Peigne S., and Schiff D., *Radiative energy loss of high-energy quarks and gluons in a finite volume quark - gluon plasma*, Nucl. Phys. **B483** (1997), 291–320, doi: 10.1016/S0550-3213(96)00553-6

[77] Baier R., Dokshitzer Y.L., Mueller A.H., Peigne S., and Schiff D., *Radiative energy loss and p(T) broadening of high-energy partons in nuclei*, Nucl. Phys. **B484** (1997), 265–282, doi: 10.1016/S0550-3213(96)00581-0

[78] Baier R., Dokshitzer Y.L., Mueller A.H., and Schiff D., *Radiative energy loss of high-energy partons traversing an expanding QCD plasma*, Phys. Rev. **C58** (1998), 1706–1713, doi: 10.1103/PhysRevC.58.1706

[79] Baier R., Dokshitzer Y.L., Mueller A.H., and Schiff D., *Medium induced radiative energy loss: Equivalence between the BDMPS and Zakharov formalisms*, Nucl. Phys. **B531** (1998), 403–425, doi: 10.1016/S0550-3213(98)00546-X

[80] Zakharov B.G., *Fully quantum treatment of the Landau-Pomeranchuk-Migdal effect in QED and QCD*, JETP Lett. **63** (1996), 952–957, doi: 10.1134/1.567126

[81] Wiedemann U.A., *Transverse dynamics of hard partons in nuclear media and the QCD dipole*, Nucl. Phys. **B582** (2000), 409–450, doi: 10.1016/S0550-3213(00)00286-8

[82] Wiedemann U.A., *Gluon radiation off hard quarks in a nuclear environment: Opacity expansion*, Nucl. Phys. **B588** (2000), 303–344, doi: 10.1016/S0550-3213(00)00457-0

[83] Wiedemann U.A., *Jet quenching versus jet enhancement: A Quantitative study of the BDMPS-Z gluon radiation spectrum*, Nucl. Phys. **A690** (2001), 731–751, doi: 10.1016/S0375-9474(01)00362-1

[84] Salgado C.A. and Wiedemann U.A., *Calculating quenching weights*, Phys. Rev. **D68** (2003), 014008, doi: 10.1103/PhysRevD.68.014008

[85] Armesto N., Salgado C.A., and Wiedemann U.A., *Medium induced gluon radiation off massive quarks fills the dead cone*, Phys. Rev. **D69** (2004), 114003, doi: 10.1103/PhysRevD.69.114003

[86] Gyulassy M., Levai P., and Vitev I., *Jet quenching in thin quark gluon plasmas. 1. Formalism*, Nucl. Phys. **B571** (2000), 197–233, doi: 10.1016/S0550-3213(99)00713-0

[87] Gyulassy M., Levai P., and Vitev I., *Reaction operator approach to nonAbelian energy loss*, Nucl. Phys. **B594** (2001), 371–419, doi: 10.1016/S0550-3213(00)00652-0

[88] Gyulassy M., Levai P., and Vitev I., *NonAbelian energy loss at finite opacity*, Phys. Rev. Lett. **85** (2000), 5535–5538, doi: 10.1103/PhysRevLett.85.5535

[89] Gyulassy M., Levai P., and Vitev I., *Jet tomography of Au+Au reactions including multigluon fluctuations*, Phys. Lett. **B538** (2002), 282–288, doi: 10.1016/S0370-2693(02)01990-1

[90] Qiu J.w. and Sterman G.F., *Power corrections in hadronic scattering. 1. Leading 1/Q**2 corrections to the Drell-Yan cross-section*, Nucl. Phys. **B353** (1991), 105–136, doi: 10.1016/0550-3213(91)90503-P

[91] Qiu J.w. and Sterman G.F., *Power corrections to hadronic scattering. 2. Factorization*, Nucl. Phys. **B353** (1991), 137–164, doi: 10.1016/0550-3213(91)90504-Q

[92] Luo M., Qiu J.w., and Sterman G.F., *Anomalous nuclear enhancement in deeply inelastic scattering and photoproduction*, Phys. Rev. **D50** (1994), 1951–1971, doi: 10.1103/PhysRevD.50.1951

[93] Wang X.N. and Guo X.f., *Multiple parton scattering in nuclei: Parton energy loss*, Nucl. Phys. **A696** (2001), 788–832, doi: 10.1016/S0375-9474(01)01130-7

[94] Wang E. and Wang X.N., *Jet tomography of dense and nuclear matter*, Phys. Rev. Lett. **89** (2002), 162301, doi: 10.1103/PhysRevLett.89.162301

[95] Majumder A., Wang E., and Wang X.N., *Modified dihadron fragmentation functions in hot and nuclear matter*, Phys. Rev. Lett. **99** (2007), 152301, doi: 10.1103/PhysRevLett.99.152301

[96] Arnold P.B., Moore G.D., and Yaffe L.G., *Photon emission from ultrarelativistic plasmas*, JHEP **11** (2001), 057, doi: 10.1088/1126-6708/2001/11/057

[97] Arnold P.B., Moore G.D., and Yaffe L.G., *Photon emission from quark gluon plasma: Complete leading order results*, JHEP **12** (2001), 009, doi: 10.1088/1126-6708/2001/12/009

[98] Arnold P.B., Moore G.D., and Yaffe L.G., *Photon and gluon emission in relativistic plasmas*, JHEP **06** (2002), 030, doi: 10.1088/1126-6708/2002/06/030

[99] Jeon S. and Moore G.D., *Energy loss of leading partons in a thermal QCD medium*, Phys. Rev. **C71** (2005), 034901, doi: 10.1103/PhysRevC.71.034901

[100] Turbide S., Gale C., Jeon S., and Moore G.D., *Energy loss of leading hadrons and direct photon production in evolving quark-gluon plasma*, Phys. Rev. **C72** (2005), 014906, doi: 10.1103/PhysRevC.72.014906

[101] Majumder A. and Wang X.N., *The Dihadron fragmentation function and its evolution*, Phys. Rev. **D70** (2004), 014007, doi: 10.1103/PhysRevD.70.014007

[102] Majumder A. and Wang X.N., *Evolution of the parton dihadron fragmentation functions*, Phys. Rev. **D72** (2005), 034007, doi: 10.1103/PhysRevD.72.034007

[103] Armesto N. et al., *Comparison of Jet Quenching Formalisms for a Quark-Gluon Plasma 'Brick'*, Phys.Rev. **C86** (2012), 064904, doi: 10.1103/PhysRevC.86.064904

[104] Mehtar-Tani Y., Salgado C.A., and Tywoniuk K., *Anti-angular ordering of gluon radiation in QCD media*, Phys. Rev. Lett. **106** (2011), 122002, doi: 10.1103/PhysRevLett.106.122002

[105] Mehtar-Tani Y., Salgado C.A., and Tywoniuk K., *Jets in QCD Media: From Color Coherence to Decoherence*, Phys. Lett. **B707** (2012), 156–159, doi: 10.1016/j.physletb.2011.12.042

[106] Casalderrey-Solana J., Mehtar-Tani Y., Salgado C.A., and Tywoniuk K., *New picture of jet quenching dictated by color coherence*, Phys. Lett. **B725** (2013), 357–360, doi: 10.1016/j.physletb.2013.07.046

[107] Blaizot J.P., Iancu E., and Mehtar-Tani Y., *Medium-induced QCD cascade: democratic branching and wave turbulence*, Phys. Rev. Lett. **111** (2013), 052001, doi: 10.1103/PhysRevLett.111.052001

[108] Spousta M., *Overview of new results from ATLAS heavy ion physics program*, Nucl. Part. Phys. Proc. **23** (2016), 28, doi: 10.1016/j.nuclphysbps.2016.05.006

[109] Aad G. et al., *Centrality and rapidity dependence of inclusive jet production in* $\sqrt{s_{\mathrm{NN}}}$ *= 5.02 TeV proton–lead collisions with the ATLAS detector*, Phys. Lett. **B748** (2015), 392–413, doi: 10.1016/j.physletb.2015.07.023

[110] Eskola K.J., Paukkunen H., and Salgado C.A., *EPS09: A New Generation of NLO and LO Nuclear Parton Distribution Functions*, JHEP **04** (2009), 065, doi: 10.1088/1126-6708/2009/04/065

[111] Aad G. et al., *Measurement of the dependence of transverse energy production at large pseudorapidity on the hard-scattering kinematics of proton-proton collisions at* $\sqrt{s} = 2.76$ *TeV with ATLAS*, Phys. Lett. **B756** (2016), 10–28, doi: 10.1016/j.physletb.2016.02.056

[112] Armesto N., Glhan D.C., and Milhano J.G., *Kinematic bias on centrality selection of jet events in pPb collisions at the LHC*, Phys. Lett. **B747** (2015), 441–445, doi: 10.1016/j.physletb.2015.06.032

[113] Aad G. et al., *Z Boson Production in p+Pb Collisions at* $\sqrt{s_{\mathrm{NN}}} = 5.02$ *TeV with the ATLAS Detector*, ATLAS-CONF-2014-020 (2014)

[114] Perepelitsa D.V. and Steinberg P.A., *Calculation of centrality bias factors in p+A collisions based on a positive correlation of hard process yields with underlying event activity*, arXiv:1412.0976 (2014)

[115] Guzey V. and Strikman M., *Proton-nucleus scattering and cross section fluctuations at RHIC and LHC*, Phys. Lett. **B633** (2006), 245–252, doi: 10.1016/j.physletb.2005.11.065,10.1016/j.physletb.2008.04.010, [Erratum: Phys. Lett.,B663,456(2008)]

[116] Alvioli M. and Strikman M., *Color fluctuation effects in proton-nucleus collisions*, Phys. Lett. **B722** (2013), 347–354, doi: 10.1016/j.physletb.2013.04.042

[117] Aad G. et al., *Measurement of differential* J/ψ *production cross sections and forward-backward ratios in p + Pb collisions with the ATLAS detector*, Phys. Rev. **C92** (2015), 034904, doi: 10.1103/PhysRevC.92.034904

[118] Aad G. et al., *Study of J/ψ and ψ(2S) production in $\sqrt{s_{\rm NN}}$ = 5.02 TeV p + Pb and $\sqrt{s}$ = 2.76 TeV pp collisions with the ATLAS detector*, ATLAS-CONF-2015-023 (2015)

[119] Cacciari M. et al., *Theoretical predictions for charm and bottom production at the LHC*, JHEP **10** (2012), 137, doi: 10.1007/JHEP10(2012)137

[120] Aad G. et al., *Transverse Momentum Dependance of Charged Particle Production in p+Pb $\sqrt{s_{\rm NN}}$ = 5.02 TeV collisions measured by ATLAS experiment at the LHC*, ATLAS-CONF-2013-107 (2013)

[121] Aad G. et al., *Jet Fragmentation in p+Pb Collisions*, ATLAS-CONF-2015-022 (2015)

[122] Aad G. et al., *Observation of Associated Near-Side and Away-Side Long-Range Correlations in $\sqrt{s_{NN}}$=5.02TeV Proton-Lead Collisions with the ATLAS Detector*, Phys. Rev. Lett. **110** (2013), 182302, doi: 10.1103/PhysRevLett.110.182302

[123] Aad G. et al., *Measurement with the ATLAS detector of multi-particle azimuthal correlations in p+Pb collisions at $\sqrt{s_{NN}}$=5.02 TeV*, Phys. Lett. **B725** (2013), 60–78, doi: 10.1016/j.physletb.2013.06.057

[124] Aad G. et al., *Measurement of long-range pseudorapidity correlations and azimuthal harmonics in $\sqrt{s_{\rm NN}}$ = 5.02 TeV proton-lead collisions with the ATLAS detector*, Phys.Rev. **C90** (2014), 044906, doi: 10.1103/PhysRevC.90.044906

[125] Aad G. et al., *Centrality, rapidity and transverse momentum dependence of isolated prompt photon production in lead-lead collisions at $\sqrt{s_{\rm NN}}$ = 2.76 TeV measured with the ATLAS detector*, Phys. Rev. **C93** (2016), 034914, doi: 10.1103/PhysRevC.93.034914

[126] Aad G. et al., *Measurement of the production and lepton charge asymmetry of W bosons in Pb+Pb collisions at $\sqrt{\mathbf{s_{NN}}}$ = **2.76 TeV** with the ATLAS detector*, Eur.Phys.J. **C75** (2015), 23, doi: 10.1140/epjc/s10052-014-3231-6

[127] Aad G. et al., *Measurement of Z boson Production in Pb+Pb Collisions at $\sqrt{s_{NN}}$ = 2.76 TeV with the ATLAS Detector*, Phys. Rev. Lett. **110** (2013), 022301, doi: 10.1103/PhysRevLett.110.022301

[128] Catani S., Fontannaz M., Guillet J.P., and Pilon E., *Cross-section of isolated prompt photons in hadron hadron collisions*, JHEP **05** (2002), 028, doi: 10.1088/1126-6708/2002/05/028

[129] Lai H.L. et al., *New parton distributions for collider physics*, Phys. Rev. **D82** (2010), 074024, doi: 10.1103/PhysRevD.82.074024

[130] Kolb P.F. and Heinz U.W., *Hydrodynamic description of ultrarelativistic heavy ion collisions*, nucl-th/0305084 (2003)

[131] Luzum M. and Romatschke P., *Conformal Relativistic Viscous Hydrodynamics: Applications to RHIC results at s(NN)**(1/2) = 200-GeV*, Phys. Rev. **C78** (2008), 034915, doi: 10.1103/PhysRevC.78.034915,10.1103/PhysRevC.79.039903, [Erratum: Phys. Rev.C79,039903(2009)]

[132] Aad G. et al., *Measurement of the pseudorapidity and transverse momentum dependence of the elliptic flow of charged particles in lead-lead collisions at* $\sqrt{s_{NN}} = 2.76$ *TeV with the ATLAS detector*, Phys. Lett. **B707** (2012), 330–348, doi: 10.1016/j.physletb.2011.12.056

[133] Aad G. et al., *Measurement of the azimuthal anisotropy for charged particle production in* $\sqrt{s_{NN}} = 2.76$ *TeV lead-lead collisions with the ATLAS detector*, Phys. Rev. **C86** (2012), 014907, doi: 10.1103/PhysRevC.86.014907

[134] Aad G. et al., *Measurement of the centrality and pseudorapidity dependence of the integrated elliptic flow in lead-lead collisions at* $\sqrt{s_{\rm NN}} = 2.76$ *TeV with the ATLAS detector*, Eur. Phys. J. **C74** (2014), 2982, doi: 10.1140/epjc/s10052-014-2982-4

[135] Aad G. et al., *Measurement of flow harmonics with multi-particle cumulants in Pb+Pb collisions at* $\sqrt{s_{\rm NN}} = 2.76$ *TeV with the ATLAS detector*, Eur. Phys. J. **C74** (2014), 3157, doi: 10.1140/epjc/s10052-014-3157-z

[136] Aad G. et al., *Measurement of the distributions of event-by-event flow harmonics in lead-lead collisions at = 2.76 TeV with the ATLAS detector at the LHC*, JHEP **11** (2013), 183, doi: 10.1007/JHEP11(2013)183

[137] Aad G. et al., *Measurement of event-plane correlations in* $\sqrt{s_{NN}} = 2.76$ *TeV lead-lead collisions with the ATLAS detector*, Phys. Rev. **C90** (2014), 024905, doi: 10.1103/PhysRevC.90.024905

[138] Aad G. et al., *Measurement of the correlation between flow harmonics of different order in lead-lead collisions at* $\sqrt{s_{NN}}$*=2.76 TeV with the ATLAS detector*, Phys. Rev. **C92** (2015), 034903, doi: 10.1103/PhysRevC.92.034903

[139] Aad G. et al., *Measurement of two-particle pseudorapidity correlations in lead-lead collisions at* $\sqrt{s_{NN}}$ *= 2.76 TeV with the ATLAS detector*, ATLAS-CONF-2015-020 (2015)

[140] Spousta M., *Jet results and jet reconstruction techniques in p + p and their prospects in heavy-ion collisions in ATLAS*, Int. J. Mod. Phys. **E20** (2011), 1545–1550, doi: 10.1142/S0218301311019842

[141] Aad G. et al., *Transverse energy fluctuations in Pb+Pb collisions at* $\sqrt{s_{NN}}$*=2.76 TeV with the ATLAS detector at the LHC*, ATLAS-CONF-2012-045 (2012)

[142] Spousta M., *The influence of the underlying event on jet measurements in heavy ion collisions*, J. Phys. Conf. Ser. **270** (2011), 012013, doi: 10.1088/1742-6596/270/1/012013

[143] Spousta M., *Jet physics in Pb-Pb collisions with ATLAS*, PoS **2008LHC** (2008), 091

6 Publications forming habilitation thesis

6.1 Experimental studies of jets in proton-proton collisions

In this section, I collect publications on experimental studies of jets in proton-proton collisions where I'm one main of authors within the ATLAS Collaboration.

- Aad G. et al., *Measurement of inclusive jet and dijet cross sections in proton-proton collisions at 7 TeV centre-of-mass energy with the ATLAS detector*, Eur. Phys. J. **C71** (2011), 1512, doi: 10.1140/epjc/s10052-010-1512-2
- Aad G. et al., *Study of Jet Shapes in Inclusive Jet Production in pp Collisions at* $\sqrt{s} = 7$ *TeV using the ATLAS Detector*, Phys. Rev. **D83** (2011), 052003, doi: 10.1103/PhysRevD.83.052003
- Spousta M., *Jet results and jet reconstruction techniques in p + p and their prospects in heavy-ion collisions in ATLAS*, Int. J. Mod. Phys. **E20** (2011), 1545–1550, doi: 10.1142/S0218301311019842

6.2 Experimental studies of jets in heavy ion collisions

In this section, five publications on experimental results from heavy ion collisions are collected where I'm one of up to eight main authors within the ATLAS Collaboration. Also included are two conference notes which were done with my significant contribution. These two conference notes contain interesting results which will likely not be submitted to a journal due to technical constraints or simply due to our decision to work on other topics. Then, I include two (out of about 16) proceeding papers which summarize some of problems that we met during the preparations for the heavy ion run. The last publication in this section is an invited review written for journal Modern Physics Letters A.

- Aad G. et al., *Observation of a Centrality-Dependent Dijet Asymmetry in Lead-Lead Collisions at* $\sqrt{s_{NN}} = 2.77$ *TeV with the ATLAS Detector at the LHC*, Phys. Rev. Lett. **105** (2010), 252303, doi: 10.1103/PhysRevLett.105.252303

- Aad G. et al., *Measurement of the jet radius and transverse momentum dependence of inclusive jet suppression in lead-lead collisions at* $\sqrt{s_{NN}}$*= 2.76 TeV with the ATLAS detector*, Phys. Lett. **B719** (2013), 220–241, doi: 10.1016/j.physletb.2013.01.024

- Aad G. et al., *Measurement of inclusive jet charged-particle fragmentation functions in Pb+Pb collisions at* $\sqrt{s_{NN}} = 2.76$ *TeV with the ATLAS detector*, Phys. Lett. **B739** (2014), 320–342, doi: 10.1016/j.physletb.2014.10.065

- Aad G. et al., *Measurements of the Nuclear Modification Factor for Jets in Pb+Pb Collisions at* $\sqrt{s_{\mathrm{NN}}} = 2.76$ *TeV with the ATLAS Detector*, Phys. Rev. Lett. **114** (2015), 072302, doi: 10.1103/PhysRevLett.114.072302

- Aad G. et al., *Measurement of the production of neighbouring jets in lead-lead collisions at* $\sqrt{s_{\mathrm{NN}}} = 2.76$ *TeV with the ATLAS detector*, Phys. Lett. **B751** (2015), 376–395, doi: 10.1016/j.physletb.2015.10.059

- Aad G. et al., *Transverse energy fluctuations in Pb+Pb collisions at* $\sqrt{s_{NN}}$*=2.76 TeV with the ATLAS detector at the LHC*, ATLAS-CONF-2012-045 (2012)

- Aad G. et al., *Jet energy scale and its uncertainty for jets reconstructed using the ATLAS heavy ion jet algorithm*, ATLAS-CONF-2015-016 (2015)

- Spousta M., *The influence of the underlying event on jet measurements in heavy ion collisions*, J. Phys. Conf. Ser. **270** (2011), 012013, doi: 10.1088/1742-6596/270/1/012013

- Spousta M., *Jet physics in Pb-Pb collisions with ATLAS*, PoS **2008LHC** (2008), 091

- Spousta M., *Jet Quenching at LHC*, Mod. Phys. Lett. **A28** (2013), 1330017, doi: 10.1142/S0217732313300176

6.3 Technical aspects of jet reconstruction in busy environment

In this section two publications on technical aspects of jet reconstruction in proton-proton and heavy ion collisions are collected. The first one is a part of a large publication on the jet triggering in the LHC run 1 (the part on the triggering in *pp* collisions is omitted). The second one is a publication on the method for the subtraction of large backgrounds from jets at the level of jet constituents.

- Aad G. et al., *The performance of the jet trigger for the ATLAS detector during 2011 data taking*, Eur. Phys. J. **C76** (2016), 526, doi: 10.1140/epjc/s10052-016-4325-0
- Berta P., Spousta M., Miller D.W., and Leitner R., *Particle-level pileup subtraction for jets and jet shapes*, JHEP **1406** (2014), 092, doi: 10.1007/JHEP06(2014)092

6.4 Phenomenological studies of jet quenching

In this section I collect two publications on phenomenological studies of the jet quenching. The first one extracts the magnitude of the parton energy loss and explains a peculiar behavior of the enhancement of the production of particles with large momentum fractions in jets seen in heavy ion collisions. The second one quantifies the difference in the radiation of quark and gluon jets between the vacuum and deconfined medium. Further, it elaborates on a connection between the jet quenching and charmonia suppression.

- Spousta M. and Cole B., *Interpreting single jet measurements in Pb + Pb collisions at the LHC*, Eur. Phys. J. **C76** (2016), 50, doi: 10.1140/epjc/s10052-016-3896-0
- Spousta M., *On similarity of jet quenching and charmonia suppression*, Phys. Lett. **B767** (2017), 10–15, doi: 10.1016/j.physletb.2017.01.041